

## Paleoenvironmental changes during sapropel 19 (i-cycle 90) deposition: Evidences from geochemical, mineralogical and micropaleontological proxies in the mid-Pleistocene Montalbano Jonico land section (southern Italy)

Patrizia Maiorano <sup>a,\*</sup>, Giuseppe Aiello <sup>b</sup>, Diana Barra <sup>b</sup>, Paola Di Leo <sup>c</sup>,  
Sebastien Joannin <sup>d</sup>, Fabrizio Lirer <sup>e</sup>, Maria Marino <sup>a</sup>, Anna Pappalardo <sup>c</sup>,  
Lucilla Capotondi <sup>f</sup>, Neri Ciaranfi <sup>a</sup>, Simona Stefanelli <sup>a</sup>

<sup>a</sup> Dipartimento di Geologia e Geofisica, Università di Bari, via E. Orabona 4, 70125 Bari, Italy

<sup>b</sup> Dipartimento di Scienze della Terra, Università di Napoli "Federico II", Largo San Marcellino 10, 80138 Napoli, Italy

<sup>c</sup> Istituto di Metodologie per l'Analisi Ambientale, CNR, C.da S. Loja- Zona Ind.le Tito Scalo, 85050 Tito Scalo (PZ), Italy

<sup>d</sup> Université Claude Bernard Lyon 1 Bat. GEODE: 2 rue Dubois 43 Bd du 11 Nov. 1918, 69622 Villeurbanne Cedex, France

<sup>e</sup> Istituto Ambiente Marino Costiero (IAMC), CNR, Calata Porta di Massa, 80133 Napoli, Italy

<sup>f</sup> Istituto di Scienze Marine, CNR, via Gobetti 101, 40129 Bologna, Italy

Received 22 May 2007; received in revised form 10 October 2007; accepted 12 October 2007

### Abstract

An integrated micropaleontological, geochemical and mineralogical study has been performed across the mid-Pleistocene sapropel 19 (i-cycle 90) from the Montalbano Jonico land section (southern Italy), to reconstruct the paleoenvironmental conditions at time of its formation. The sapropel interval is characterized by two oxygen depletion phases (phase A and C) interrupted by a temporary re-oxygenation interval (phase B). The beginning and the end of sapropel deposition are dated at  $957 \pm 0.81$  kyr and  $950 \pm 0.86$  kyr respectively. The duration of the interruption is estimated to  $0.350 \pm 0.32$  kyr. The multiproxy approach highlights that deposition of sapropel 19 reflects a period of enhanced freshwater runoff induced by a wetter climate. As a consequence of a more efficient fluvial erosion, a higher terrigenous input, mostly ascribable to a southern Apennines source, and an increased turbidity of surface waters accompanied most of sapropel deposition. Biotic and abiotic proxies document that different paleoenvironmental conditions occur through phases A–C. The beginning of phase A is characterized by warm on-land paleoclimate as well as warm and oligotrophic surface water conditions. During the upper part of phase A temperature starts decreasing and surface waters appear more productive. This change probably represents the prelude to cooler and drier conditions characterizing phase B, which displays a river supply reduction and an eolian input increase (Sahara dust). During phase C the restored depleted oxygen environment at the bottom sediments is clearly coupled with the re-establishment of humid conditions and increased river supply. At the same time, enhanced mixing of water column, a cooler paleoclimate, and increased productivity of surface waters are recorded, the latter likely favored by the enhanced mixing of water column and also increased delivery of land-derived nutrients. The end of phase C is marked by a restored "normal" run-off. Enhanced productivity in surface waters and low oxygen conditions at the bottom sediments persist slightly above phase C. The overall results suggest that the onset of sapropel deposition is related to water stratification that caused low oxygen

\* Corresponding author. Fax: +39 080 5442625.

E-mail address: [p.maiorano@geo.uniba.it](mailto:p.maiorano@geo.uniba.it) (P. Maiorano).

exchanges with the sea-bottom. Although enhanced productivity characterizes most of the sapropel deposition it was not the primary factor triggering sapropel deposition.

© 2007 Elsevier B.V. All rights reserved.

**Keywords:** Sapropel 19; Southern Italy; Geochemistry and mineralogy; Micropaleontology; Mid-Pleistocene

### 1. Introduction

Sapropel layers represent a particular feature of the Neogene Mediterranean sedimentary record (Robertson et al., 1998). They consist of dark-colored, laminated sediments enriched in organic carbon and are interbedded in the normal sediments of the Mediterranean basin. It is widely accepted that cyclic occurrence of sapropels in the depositional record is the expression of orbitally forced paleoclimate and paleoceanographic changes. They correspond in fact to minima in the earth’s orbital precessional cycle and insolation maxima (Rossignol-Strick, 1985; Hilgen, 1991; Hilgen et al., 1997), which were periods of wetter climate (Rossignol-Strick, 1983; Rohling and Hilgen 1991). However, it is

still controversial how the sea water column responds to such a global climatic change and leads to sapropel formation. According to some of the most corroborated hypotheses, the increased freshwater runoff is believed to drive near-surface stratification and therefore to decrease vertical circulation of water column, thus leading to anoxic conditions at the sea floor and consequent organic matter preservation (e.g. Olausson, 1961; Thunell, 1979; Vergnaud-Grazzini, 1985). Other authors (De Lange and Ten Haven, 1983; Calvert, 1983; Pedersen and Calvert, 1990) consider enhanced primary production in the photic zone, induced by river-derived nutrients, to be the primary cause of the increased accumulation of organic matter in the seafloor and hence the major cause of sapropel deposition. Moreover, a

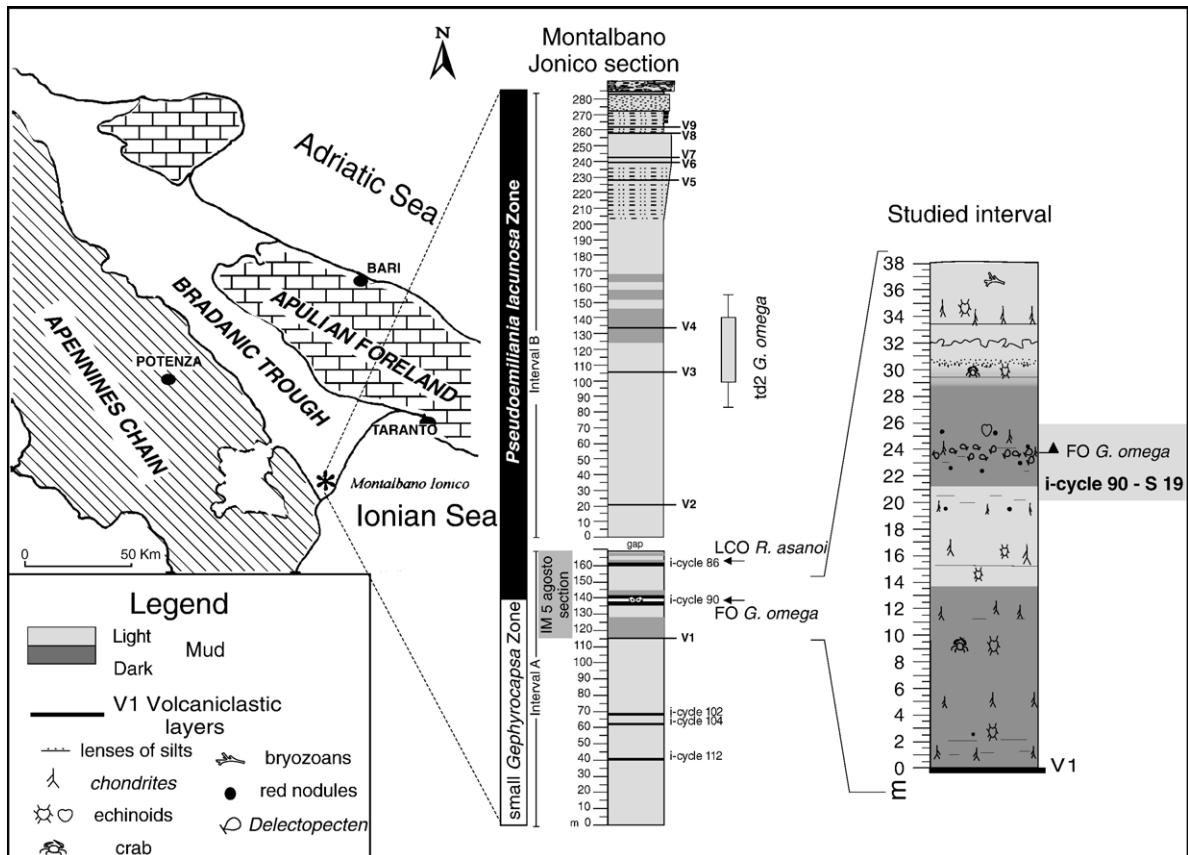


Fig. 1. Location, lithology and main stratigraphical features of the composite Montalbano Jonico section and of the IM-5 agosto section.

combination of enhanced primary production and density stratification has also been invoked to explain sapropel formation (Rohling and Gieskes, 1989; Rohling, 1991; Rohling and Hilgen, 1991; Howell and Thunell, 1992).

Despite their controversial origin, a century to millenium-scale interruption of some sapropel layers, which indicates short temporary interruption of the conditions favouring their formation, is a well documented aspect of sapropel deposition (Thunell et al., 1977; Cita et al., 1984; Rohling et al., 1993; De Rijk et al., 1999; Mercone et al., 2001; Arnaboldi and Meyers, 2003; Hassold et al., 2003; Meyers and Bernasconi, 2005). Repopulation of benthic foraminifera, as well as low organic carbon content, characterize sapropel interruptions and suggest improved deep water ventilation as a consequence of the onset of abrupt cooling and/or increased aridity (Rohling et al., 1997; De Rijk et al., 1999; Myers and Rohling, 2000; Casford et al., 2001, 2003; Schmiedl et al., 2003; Sangiorgi et al., 2003). This event is supposed to be a consequence of intensification in the frequency/intensity of cold northerly air outbreaks over the basin, in relation to enhanced Siberian high pressure conditions (Rohling et al., 2002a,b). An example of an interrupted sapropel is the sapropel 19 which was deposited during insolation cycle 90. It has been recorded so far in several deep marine ODP cores (Sites 975, 974 969, 967), from the Balearic to the Levantine basins (Meyers and Arnaboldi, 2005). In land sections, the sapropel 19 is documented in the Montalbano Jonico section outcropping in southern Italy (Fig. 1), where it has been identified by means of benthic and planktic foraminiferal assemblages and  $\delta^{18}\text{O}$  record (Stefanelli et al., 2005). The high sedimentation rate of Montalbano Jonico section offers a unique opportunity to examine an expanded stratigraphic interval, thus providing a high-resolution paleoenvironmental data set.

Aiming to spread light on the paleoenvironmental picture that led to sapropel formation and to better define the mechanisms responsible for sapropel interruption, an integrated mineralogical, geochemical and micropaleontological study across the mid-Pleistocene interrupted sapropel 19 of Montalbano Jonico land section has been performed. Specifically, mineralogical and geochemical signals helped to discriminate, in the Montalbano Jonico section, different sources of sediment input and give indirect information on climate conditions which characterized sapropel and pre-/post-sapropel deposition. At the same time, micropaleontological data from calcareous nannoplankton, pollen and ostracod analyses integrated with previous data avail-

able on the same samples (Stefanelli et al., 2005) on both benthic and planktonic foraminiferal assemblages and on *Globigerina bulloides* oxygen isotope record, allowed reconstruction of the biological framework for a better understanding of the characteristics of water column and of the climate conditions at the time of sapropel deposition.

## 2. Materials and methods

### 2.1. The IM-5 agosto section

The IM-5 agosto section, which has been investigated in detail in the present study, is a partial interval of the well known Montalbano Jonico composite section (Ciaranfi et al., 2001) located in the southernmost part of the southern Apennines Foredeep (Fig. 1). The stratigraphical and paleoenvironmental framework of Montalbano Jonico composite section has been studied in great detail by several authors (Ciaranfi et al., 2001; Ciaranfi and D'Alessandro, 2005 and references therein). The investigated interval, mainly represented by hemipelagic silts and silty clays, is about 38 m thick (Fig. 1). It corresponds to the transition between the small *Gephyrocapsa/Pseudoemiliana lacunosa* Zone (Ciaranfi et al., 2001; Maiorano et al., 2004) and is indicative of an upper slope setting and a water depth of about 250–350 m (D'Alessandro et al., 2003; this study). Therefore, the variations in the characteristic of water column can be expected to reflect changes in surface and intermediate waters.

The IM-5 agosto section includes a dark, locally laminated interval, 5.6 m thick (from 20.2 m to 25.8 m) containing the First Occurrence (FO) of *Gephyrocapsa omega* dated at 0.95 Ma (Maiorano et al., 2004). This dark interval, correlated to MIS 25 and corresponding to a maximum flooding interval (D'Alessandro et al., 2003) has been associated with sapropel 19 and i-cycle 90 (Ciaranfi et al., 2001; Maiorano et al., 2004), which are orbitally tuned at 954 kyr (Lourens, 2004). High-resolution foraminiferal investigations (Stefanelli et al., 2005) identified an interrupted interval within the sapropel deposition. Two severe oxygen depletion phases, here indicated as phase A (20.2–21.8 m) and phase C (22.4–25.8 m), characterized by the *Globobulimina*-assemblage and by the *Bolivina*-assemblage respectively (Fig. 2), have been related to warming and decreasing of salinity in the surface and intermediate water layers (Stefanelli et al., 2005). The two phases are separated by a temporary re-oxygenation of the sediment pore water (phase B) characterized by a short-term benthic repopulation (Fig. 2).

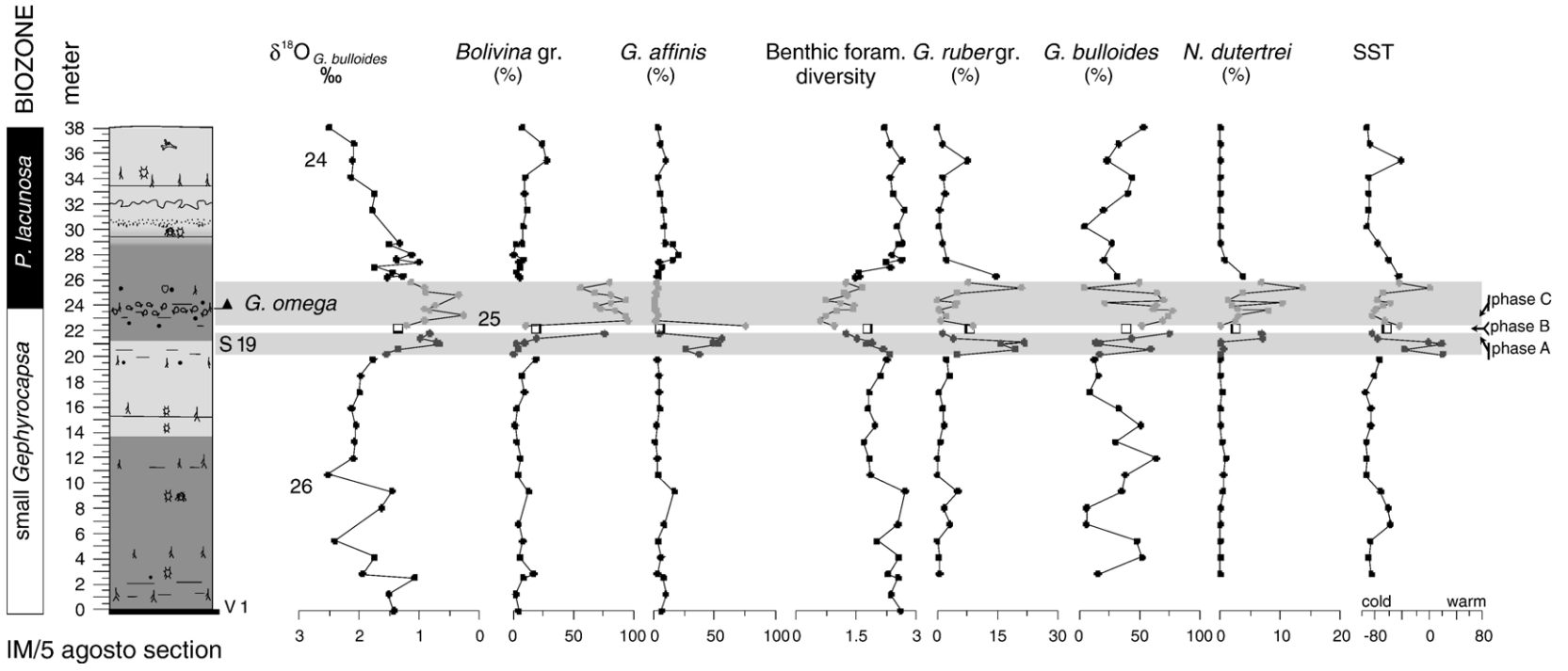


Fig. 2. Oxygen stable isotope record on *Globigerina bulloides*, selected abundance patterns of benthic and planktonic foraminifera and Sea Surface Temperature (SST) curve at the IM-5 agosto section (modified from Stefanelli et al., 2005). SST curve is based on the ratio warm versus cool planktonic foraminifera indicators following Lourens et al. (1992).

## 2.2. Sampling and analyses

The IM-5 agosto section has been sampled every 130 cm in the interval below and above the sapropel layer and every 20–40 cm within the sapropel layer and immediately above, thus providing a sampling resolution respectively of  $\sim 2.5$  kyr and  $\sim 0.6$  kyr, given a mean sedimentation rate of about 55 cm/kyr (Fig. 3).

### 2.2.1. Geochemical and mineralogical analyses

Major and trace element analyses (Appendix A), including rare earth elements (REE), of a selected number of samples from the IM-5 agosto section were performed by ICP-OES/AAS (Induced Coupled Plasma-Optical Emission/Atomic Absorption Spectroscopy) and ICP-MS (Mass Spectroscopy) analysis.

Samples for geochemical analyses were rinsed with distilled water and centrifuged to remove sea salts, and then dried at 60 °C for 24 h. Sediments were homogenized in an agate mortar. Lithium metaborate/tetraborate fusion technique was used as extraction method. Total loss on ignition (LOI) was gravimetrically estimated after overnight heating at 950 °C.

Organic carbon (wt.%) and total nitrogen (wt.%) were determined by LECO Combustion-IR technique on an automated LECO CS-344 analyzer. Specifically, organic carbon was detected according to the following procedure: an initial amount of 0.5 g of sample is titrated with 25% HCl to drive off the CO<sub>2</sub> (inorganic carbon). The sample is neutralized with ammonium hydroxide and dried on a hot plate. Sample residue is analyzed by LECO Combustion-IR technique to provide a value for total carbon, which is composed of organic and graphitic carbon. The graphitic carbon content is subtracted to provide the organic carbon content.

Biogenic silica content was calculated from ICP major-element data and by using the normative model from Robinson (1994): (biogenic silica) =  $\text{SiO}_2 - 2.8 * \text{Al}_2\text{O}_3$ . The factor 2.8 was preferred to the one often used as “average shale” silica/alumina ratio of 3.4 (Turekian and Wedepohl, 1961) because better fitting the more aluminous sediments.

The mineralogy of bulk samples and of the clay fraction (<2  $\mu\text{m}$  grain-size fraction) were determined by XRD (Rigaku miniflex, CuK $\alpha$  radiation, sample spinner) and the relative abundances of the mineralogical phases are reported in Appendix A. To identify clay minerals, a known amount of the <2  $\mu\text{m}$  grain-size fraction was crushed in a hand mortar and then transferred to a plastic container for ultrasonic treatment for 2–3 min. After settling, the suspension was decanted, pipetted, and dried at room temperature on glass slides to produce a thin-

layer, well-oriented aggregate with a particle density of at least 3 mg/cm<sup>2</sup>. Air-dried, ethylene-glycol solvated and heated (250 °C) slides were X-rayed and the X-ray patterns were used for clay minerals quantification.

Particle size analysis of the samples was carried out on a laser granulometer MasterSizer E Ver 1.2, from Malvern Instruments Ltd., Malvern, UK.

### 2.2.2. Pollen

Samples were prepared using a standard chemical technique adapted from Cour (1974). HCl and HF attacks were followed by residue sieving at 160  $\mu\text{m}$  and 10  $\mu\text{m}$  respectively and by enrichment procedures (e.g. ZnCl<sub>2</sub>). The pollen flora was documented with a minimum of 20 taxa per sample. More than 8600 pollen grains (which corresponds to at least 150 grains per sample) were counted besides *Pinus*, since it is generally over-represented in marine sediments (Heusser, 1988; Beaudouin et al., 2007).

### 2.2.3. Calcareous nannofossils

Smear slides were prepared from unprocessed samples using standard methodologies (Bown and Young, 1998) and analysed under a polarized light microscope at 1000x magnification. Quantitative data were collected by counting 300 nannofossils >4  $\mu\text{m}$  in size. Further, in order to evaluate the abundances of *Florisphaera profunda* with respect to all other species – as suggested by Matsuoka and Okada (1989) and Castradori (1993) – and of small placoliths <4  $\mu\text{m}$  in size, a supplementary counting of these taxa has been performed on 300 specimens of the total nannofossil assemblages. The diversity index (Shannon–Weaver index) has been estimated on the total assemblage >4  $\mu\text{m}$ .

### 2.2.4. Ostracods

Samples (300 g — dried weight) were disaggregated and washed with water through 230 and 120 mesh sieves (63  $\mu\text{m}$  and 125  $\mu\text{m}$  respectively). All the ostracods were picked from the coarsest fraction (>125  $\mu\text{m}$ ). Both number of valves and number of specimens have been counted. Number of valves includes all the recovered juvenile and adult valves. The minimum number of individuals has been calculated by adding the greater number between right and left adult valves to the number of adult carapaces. When only instars occur, the number of specimens equals to one. Ostracod abundance (OA<sub>i</sub>: number of individuals/100 g; OA<sub>v</sub>: number of valves/100 g), Shannon–Weaver diversity index (SH), Simpson’s index of diversity (S1-D) and abundance values of selected taxa have been calculated for paleoecological interpretations.

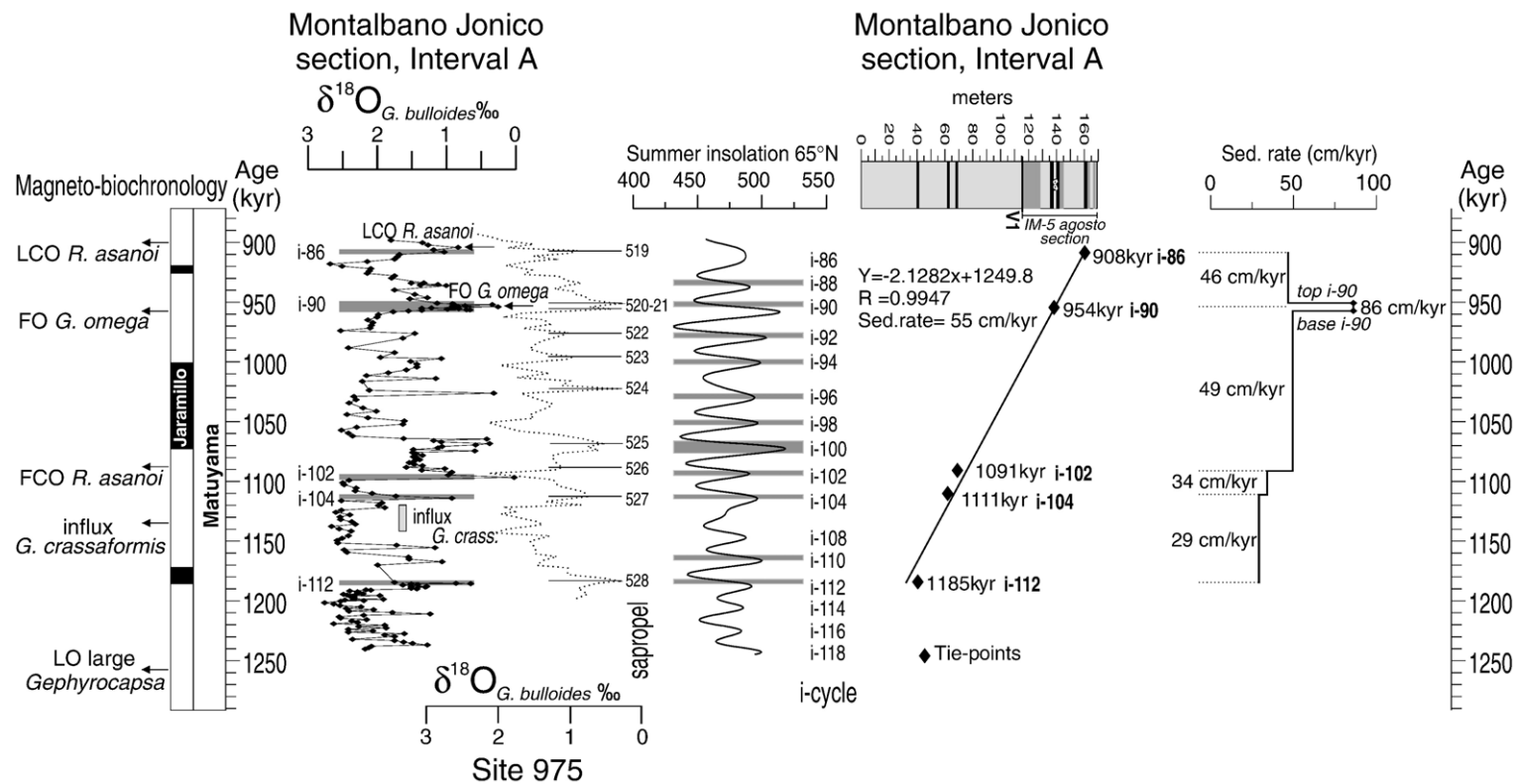


Fig. 3. Age model for  $\delta^{18}\text{O}_{G. bulloides}$  record of Montalbano Jonico section Interval A correlated to oxygen isotope and sapropel chronology of ODP Site 975 (Lourens, 2004) and to the 65°N summer insolation target curve of Laskar et al. (2004). Age–depth plot using midpoints of sapropel layers as calibration points and sedimentation rate profile with correction to the duration of sapropel 19 as described in the text are shown on the right side. Magneto-biochronology and sapropel chronology are from Lourens (2004 and reference therein). Nannofossil events at Montalbano Jonico section from Maiorano et al. (2004), influx of *G. crassaformis* from Joannin (2007). FO: First Occurrence, LO: Last occurrence, FCO: First Common Occurrence, LCO: Last Common Occurrence.

In order to perform a correct paleoenvironmental interpretation of the IM-5 agosto section, it has been necessary to discriminate autochthonous from allochthonous assemblages. Due to their small and delicate shell, and to the presence of different instars (moult), a detailed study of ostracod specimens allows in fact to recognize allochthony. Criteria commonly used to identify displacement include combined investigations on adults/instars ratio, state of preservation and depth distribution (van Harten, 1986; Brouwers, 1988). In the studied section, taxa such as *Aurila*, *Leptocythere*, *Loxoconcha*, *Semicytherura* and *Urocythereis* have been considered as displaced from the shelf. They are mainly represented by juveniles and their state of preservation is generally poor. On the contrary, specimens of *Argilloecia*, *Cytheropteron*, *Krithe* and *Parakrithe* among others, despite the fragility of their shell, are mainly in an excellent state of preservation and frequently show both adults and young instars, typical of autochthonous specimens. Paleoenvironmental interpretations are based exclusively on the latter group including genera and species sharing comparable paleobathymetric distributions and ecological requirements.

### 3. Results

#### 3.1. Time framework

Astronomical calibration of the Montalbano Jonico section interval A, which contains the IM-5 agosto section (Fig. 1), is based on the occurrence of distinct sapropel layers, that correspond to Pleistocene insolation cycles 112, 104, 102, 90 and 86 dated by Lourens (2004, and references therein). The identification of sapropel layers and their location as well, are based on the drastic increase of low oxygen tolerant benthic foraminiferal fauna (*Globobulimina affinis* and *Bolivina* gr. assemblage) (see for details Ciaranfi et al., 2001; Stefanelli, 2004; Stefanelli et al., 2005) and on planktonic  $\delta^{18}\text{O}_{G. \text{bulloides}}$  lighter values (Stefanelli et al., 2005). These sapropel layers are biostratigraphically constrained by calcareous nannofossil events (Maiorano et al., 2004) and by the recognition of the *Globorotalia crassaformis* influx (Joannin, 2007) (Fig. 3).

Following Lourens et al. (1996) and Lourens (2004), the Montalbano Jonico section interval A has been astronomically calibrated using a 3 kyr time lag between the midpoints of each sapropels and their correlative precession minima to construct the planktonic  $\delta^{18}\text{O}$  time series. On this basis, at the IM-5 agosto section, the beginning of sapropel 19 deposition would be dated at

$958 \pm 0.80$  kyr and assuming a constant and linear sedimentation rates of 49 cm/kyr the termination reaches an age of  $942 \pm 0.81$  kyr. The estimated time interval of interruption at the IM-5 agosto section is  $0.485 \pm 0.32$  kyr. Conversely, in the Balearic, Tyrrhenian and Levantine deep-sea basins sapropel 19, which was controlled by a strong peak in summer insolation  $65^\circ$  N curve, is commonly only few centimetres thick and ranges in age from about 960.5 kyr to 954 kyr (Hassold et al., 2003; Meyers and Arnaboldi, 2005) with an estimated duration of 6.5 kyr. The duration of the interruption varies from 2.6–2.2 kyr in the Balearic and Tyrrhenian basin to 1 kyr in the Levantine basin (Meyers and Arnaboldi, 2005).

The discrepancy observed in the timing of the bottom and top of the sapropel intervals as well as in the duration of interruption could be associated to the different tuning strategy proposed for this insolation cycle and/or to differences in the sedimentation rate at the IM-5 agosto section between sapropel 19 interval and pre- and post sapropel sediments. In the studied section, the peak expression of the insolation cycle 90 is in fact defined at the midpoints of sapropel 19 and tuned at 954 kyr (Lourens, 2004). Alternatively, Meyers and Arnaboldi (2005) define the insolation maximum of cycle 90 (tuned at 955 kyr) as the sample in which the highest total organic carbon (TOC) concentration occurs. The good match between the  $\delta^{18}\text{O}_{G. \text{bulloides}}$  record at Montalbano Jonico section interval A with the equivalent record from the Mediterranean ODP-Site 975 (re-calibrated by Lourens (2004), using sapropel chronology of core KC01B) confirms that the astronomical calibration of the Montalbano Jonico section Interval A is well-constrained at the scale of precessional cycle (Fig. 3). However, the much longer duration estimated for sapropel 19 at the IM-5 agosto section with respect to their deep-sea coeval counterparts, seems to suggest that a potential change in the sedimentation rate cannot be excluded in the studied section during the sapropel deposition.

Due to the absence of additional tie-points at the base and at the top of the sapropel layer 19, we then assumed the duration of 6.5 kyr for sapropel 19 following Meyers and Arnaboldi (2005). On this basis (also using the midpoint of sapropel 19 dated at 954 kyr; Lourens, 2004) we adjusted the linear sedimentation rate within the sapropel interval at the IM-5 agosto section (Fig. 3). We found that the base of sapropel is dated at  $957 \pm 0.81$  kyr and the top at  $950 \pm 0.86$  kyr. These new tie-points show that the sedimentation rate increased in the sapropel layer (Fig. 3) and that the duration of the interruption at the IM-5 agosto section is estimated at

0.350±0.32 kyr. As a result the linear regression which describes the age–depth relationship for the Montalbano Jonico section interval A indicates an average sedimentation rate of 55 cm/kyr (Fig. 3).

### 3.2. Grain size, mineralogy and geochemistry

#### 3.2.1. Grain size

Sediments from sapropel 19 can be classified mainly as silt (Folk, 1980, Fig. 4a). Sediment from the interrupted interval (phase B) mainly consists of mud (Folk, 1980; Fig. 4a). Pre- and post-sapropel sediments cannot be clearly discriminated and fall in the mud and silt fields from Folk ternary diagram, with some overlapping. Due to the proximal setting of the IM-5 agosto section, a high influx of sediments exhibiting mainly a silt–mud grain-size is clearly expected. The initial stage of sapropel (phase A) is characterized by a low clay/silt ratio (Fig. 4b) that sharply increases up to phase B. After the interruption, sapropel sediments from phase C exhibit again an increase in silty fraction (lower clay/silt ratio), interrupted by a spike at about 24.2 m, where the clay input briefly increases.

#### 3.2.2. Organic variables

A peculiar feature of samples from the IM-5 agosto section is the extremely low organic carbon content ( $C_{org}$  content background of about 0.05%; Appendix A).

However, despite the overall low  $C_{org}$  content, spikes exhibiting  $C_{org}$  values as high as 1% are observed at the IM-5 agosto section in both sapropel and pre/post sapropel sediments. Low  $C_{org}$  contents are commonly observed in on-land Pleistocene sapropel layers (less than 1%; Nijenhuis et al., 2001) compared to their coeval counterparts in deep-marine cores. Post-depositional processes may be responsible for the low organic carbon content observed in the sapropel intervals (Nijenhuis et al., 2001), but dilution caused by the higher sedimentation rate within the sapropel interval may have also occurred. With respect to the content of total nitrogen ( $N_{tot}$ ), this element is slightly more concentrated (in the range of 0.06–0.08%; Appendix A) in sapropel interval compared to pre- and post-sapropel sediments.  $C_{org}/N_{tot}$  ratio does not show a significant trend through the section (Fig. 5). Attention was also devoted to the behavior of biogenic silica content, because this variable may offer a (more specific) guide to past biological productivity compared to organic carbon. Biogenic silica distribution along the IM-5 agosto section (Fig. 5) exhibits a strong and sharp reduction at the initial stage of phase A and then starts to increase up to the phase B, in which the highest concentration of biogenic silica occurs. During sapropel phase C, biogenic silica contents are slightly higher than in phase A, with the only exception of a spike at about 25 m and immediately after the end of sapropel deposition.

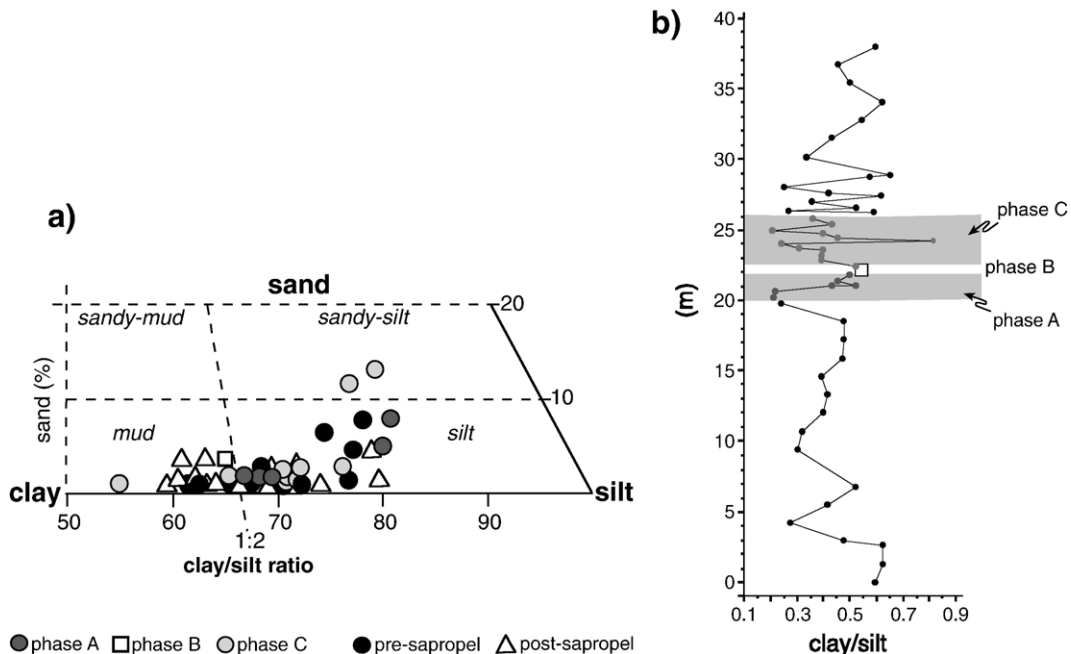


Fig. 4. a) Ternary diagram with Udden–Wentworth size class end-members and the silt-to-clay ratios (modified from Folk, 1980). b) clay-to-silt ratio variation through the IM-5 agosto section.

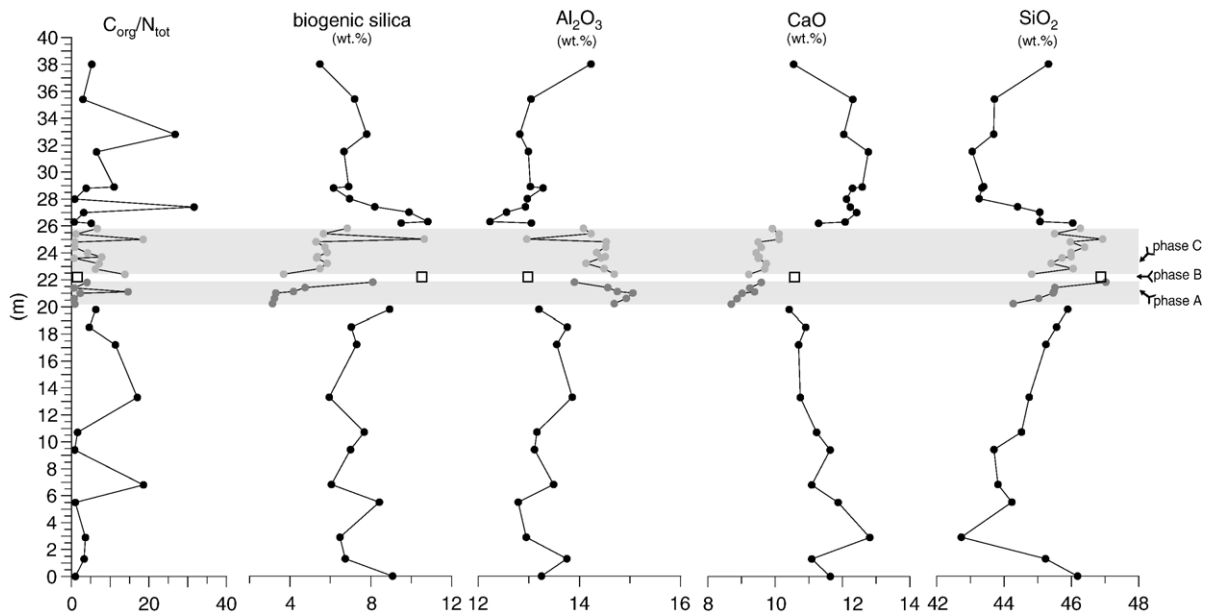


Fig. 5. Vertical distribution of major elements,  $C_{org}/N_{tot}$  and biogenic silica through the IM-5 agosto section.

### 3.2.3. Inorganic variables

The initial stage of sapropel deposition is clearly marked by a sharp increase in  $Al_2O_3$  content (Fig. 5), thus indicating an increase in the terrigenous input. This feature is observed in the whole sapropel interval with the exception of the interruption (phase B). A relative decrease in CaO as consequence of the strong dilution from clay input (high aluminium input; Fig. 5) is also observed through the sapropel layer. A sharp decrease of  $SiO_2$  characterizes the initial stage of sapropel deposition and an increase of silica content marks the upper part of phase A. A similar trend is also observed at the initial stage of phase C, with a continuum increment of  $SiO_2$  up to the top.

The chemical composition of the IM-5 agosto section sediments is also discussed in the present paper on the basis of element/Al ratios, in order to compensate for possible dilution of carbonate input. Changes in the elements/aluminum ratio distributions are observed (Fig. 6) through the sapropel layer. The Si/Al, Ti/Al,  $Mg_{(tot)}/Al$ , Ca/Al ratios are lower during phases A and C with respect to the pre-/post-sapropel sediments. This pattern, if considering the aluminum distribution in the section (14% to 15.5%, Fig. 5), is clearly consequence of the increased terrigenous supply to marine sedimentation during the time of sapropel formation. However, Ti/Al, although lower in sapropel interval with respect to the non-sapropel sediments – like the other elements/ratios shown in Fig. 6 – exhibits an increase in the final stage of phase A up to phase B. An increase of K/Al ratio is

also observed during phase B. Although Ba is considered an index of biological productivity (McManus et al., 1998 among others and reference therein), its distribution in the IM-5 agosto section does not show a significant enrichment in the sapropel interval. This feature, similarly to what previously observed by Nijenhuis et al. (2001) and Arnaboldi and Meyers (2003), supports the hypothesis that Ba/Al ratio is not a reliable paleo-productivity indicator in near-shore settings, being the shallow-water column probably responsible for the lack of the barium enrichment (Von Breymann et al., 1992). Barium excess values, calculated according to Mercone et al. (2001), show that the non-detrital Ba fraction is not preferentially accumulated in sapropel sediments, thus confirming that the low Ba/Al ratio observed in the sapropel interval at the IM-5 agosto section is not a consequence of the high aluminum concentration (Fig. 6). With respect to the redox-sensitive and chalcophile elements (Fig. 6), they are not enriched in the studied sapropel compared to pre-and post-sapropel sediments, as commonly expected for Mediterranean sapropel (Thomson et al., 1995; Nijenhuis et al., 1998 among others). This discrepancy can be a consequence of both dilution operated by the increased detrital input and increase in the sedimentation rate (Fig. 3), which does not allow a full incorporation of trace elements supplied by rivers into the sediments (Nijenhuis et al., 1999). This support the hypothesis that in sapropel 19 at the IM-5 agosto section the river input source is therefore more important than marine source in controlling the

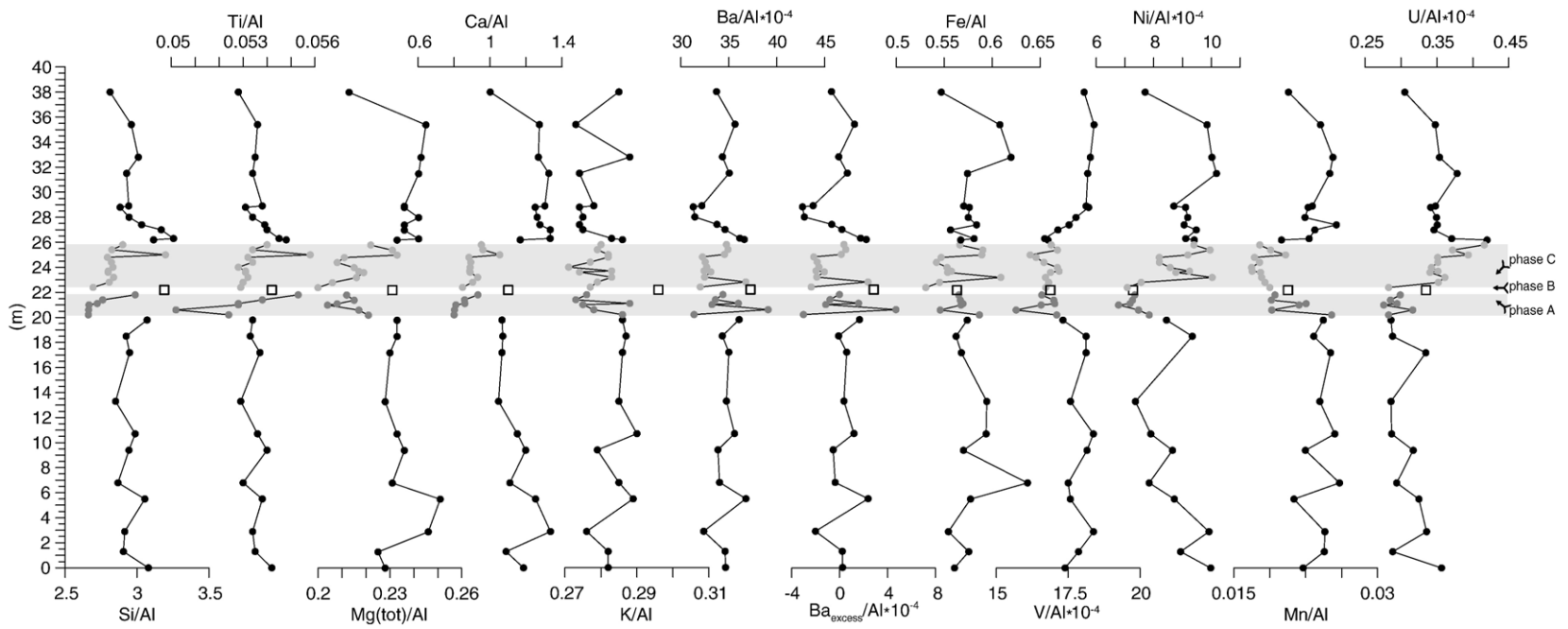


Fig. 6. Vertical distribution of selected elements/Al weight ratios through the IM-5 agostio section representative of the different groups of elements. Ba distributions are given both as normal Ba concentration/Al ratio as well as  $Ba_{\text{excess}}/Al$  ratio. For  $Ba_{\text{excess}}$  calculation  $(Ba/Al)_{\text{detrital}}$  was determined as average values from pre-and post-sapropel sediments in the IM-5 agostio section.

distribution of redox-sensitive and chalcophile elements. Further, changes in geochemical characteristics of sediment input through the entire section, i.e. changes in mafic contribution (Turekian and Wedepohl, 1961) starting from the interruption upwards, seems also to be responsible for the peculiar Ni trend and suggest that increase of this element from phase A to phase C is a feature not restricted to the sapropel interval. Despite the possible dilution and detrital input control on the redox-sensitive elements, Mn and U still appear to provide information on paleo-oxygen conditions. The trend of Mn along the entire section does not give evidence of strong diagenetic effects (Fig. 6). The Mn decrease in sapropel interval in the studied section (Fig. 6) is compatible with sediments deposited under dysoxic conditions (Mercone et al., 2001). U shows an interesting increasing trend through the sapropel (Fig. 6), reaching maximum values during the end of phase C and slightly above. This may be an indication of low-oxygen condition at the sea bottom coupled with increased productivity (Kochenov and Baturin, 2002).

#### 3.2.4. Mineralogical variables

The relative abundance of clay minerals with respect to quartz (hereafter CM/Qtz) exhibits significant variations: the initial stage of sapropel deposition is characterized by the increase of clay mineral input (high  $Al_2O_3$  content; Fig. 5), that decreases toward the end of phase A (Fig. 7). Phase B is marked by a relatively

strong decrease in quartz input and relative increase in kaolinite and feldspars (respectively highest Kaol/Qtz and lowest Kaol/[Kfs+Pl] ratios). The initial stage of phase C is characterized by a relatively low amount of clay minerals with respect to quartz (with the exclusion of a short interval between 23.7 m up to 24.2 m where a positive spike in clay minerals can be observed). The kaolinite/quartz ratio (Kaol/Qtz) also mimics, during phase A and C, the CM/Qtz as well as the kaolinite/feldspars ratios (Kaol/[Kfs+Pl]).

The relative distribution of kaolinite and chlorite (Kaol/Chl) in the clay fraction ( $<2 \mu m$ ) within the sapropel layer allows good discrimination between sapropel and homogeneous sediments: the former are characterized by a lower Kaol/Chl ratio whereas the latter shows values for this ratio higher than 1 (Fig. 7).

### 3.3. Micropaleontology

#### 3.3.1. Pollen

The pollen assemblage of the Montalbano Jonico section (see for details Joannin, 2007) is mainly composed of mesothermic elements which include trees (e.g. deciduous *Quercus*, *Carya* and *Pterocarya*) living in warm-temperate climate with wet conditions. Altitudinal elements (e.g. *Cedrus* and *Tsuga*) vary similarly to the mesothermic elements and show highest abundance during interglacials. Mesothermic, altitudinal and stepic groups are based on the cumulative percentages

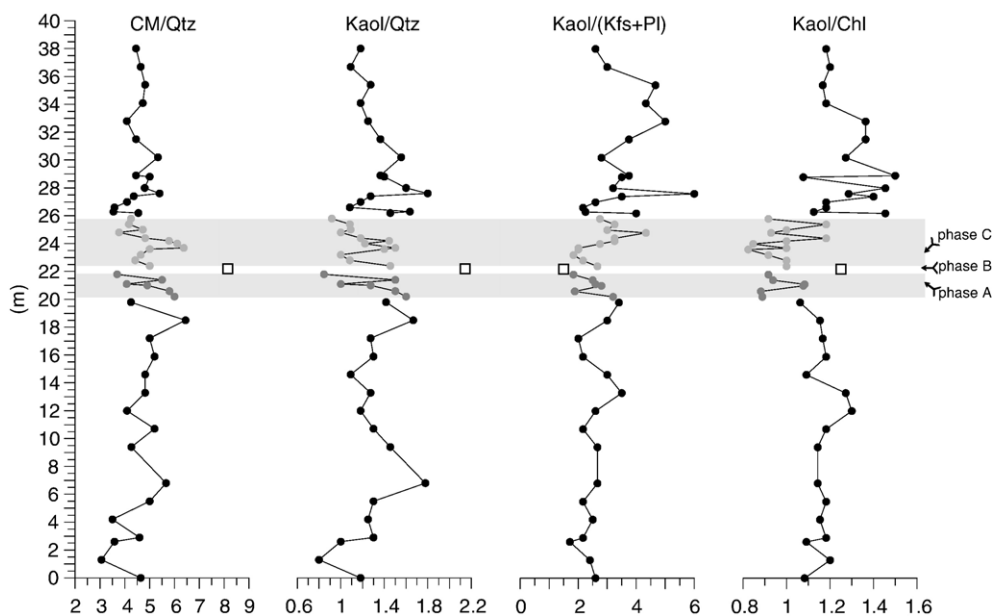


Fig. 7. Vertical distribution of mineral phase weight % ratios through the IM-5 agosto section.

of taxa according to their estimated ecology, which are defined on the basis of their representatives in the present-day plant ecosystems (Suc, 1984; Combourieu-Nebout, 1987).

Steppic elements (e.g. *Artemisia* and *Ephedra*) variations are opposite to the mesothermic elements ones. Steppic elements, which could grow in large thermic range conditions, are often linked with xeric conditions (Subally and Quézel, 2002). In the Montalbano Jonico section (Joannin, 2007), the steppic elements increases recorded cold and dry climate, like during the glacial period which precedes i-90 cycle.

Based on the observed pollen assemblage, a mesothermic vs. steppic and halophyte ratio was used to describe climatic changes in the lower part of Montalbano Jonico section (Interval A; Joannin, 2007). This ratio is also considered the most significant climate proxy for the IM-5 agosto section. In the sapropel interval, pollen analyses are characterized by a global increase of mesothermic vs. steppic and halophyte elements ratio (Fig. 8). Halophytes are able to live in saline environments and their increase is expected during sea-level falls (i.e. during glacial periods). This phenomenon has been observed in the important sea level change occurred during the Messinian crisis (Suc et al., 1995). As a consequence, high values of mesothermic vs. steppic and halophyte ratio indicate warm and wet climate. Since vegetation is

controlled by changes in temperature and precipitation with increasing altitude (Ozenda, 1975), vegetation changes described in the mesothermic vs. steppic and halophyte ratio have probably been amplified by the expansion and contraction of altitudinal vegetation belts.

Deciduous *Quercus*, belonging to the mesothermic group, has already been used to describe Mediterranean climate changes (wetness availability) in response to precession minima (Rossignol-Strick and Paterne, 1999). In the IM-5 agosto section the deciduous *Quercus* pattern mimics the mesothermic vs. steppic and halophyte elements ratio with lower frequency variations.

In the sapropel layers, the pollen ratio and deciduous *Quercus* record a sharp increasing of wet and warmer conditions in phase A, followed by a brief cooler and drier climate (phase B). As values of the pollen ratio and percentages of deciduous *Quercus* recorded during phase B are similar with values and percentages recorded during the glacial phase (MIS 26) (Fig. 8), dryness and temperature should be equivalent. On the whole, phase C is characterized by warm and wet conditions.

### 3.3.2. Calcareous nannofossils

The calcareous nannofossil assemblages are abundant and moderately preserved. The quantitative pattern of the most representative taxa are reported in Fig. 9 and compared with the most significant planktonic

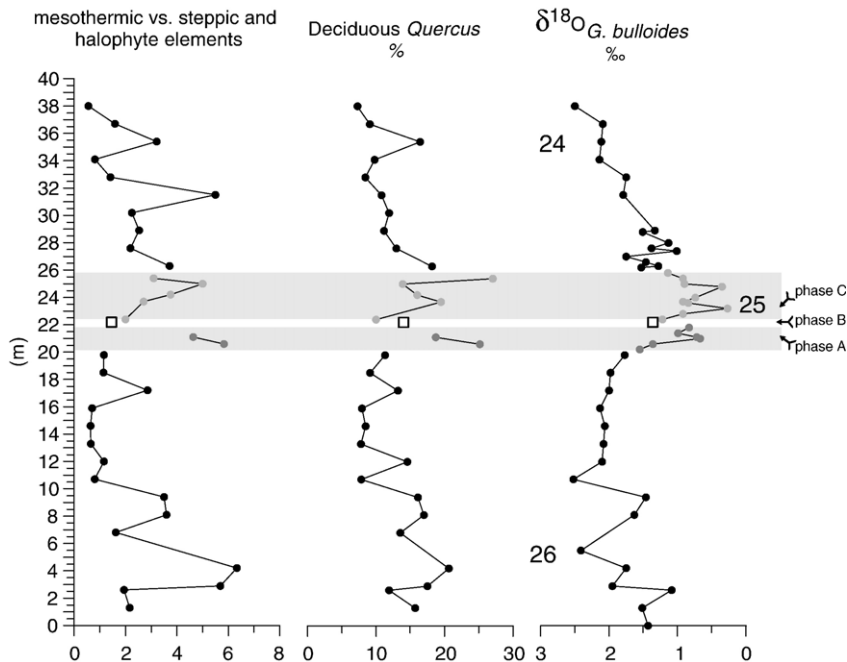


Fig. 8. Mesothermic (e.g. deciduous *Quercus*, *Carya* and *Pterocarya*) vs. steppic (e.g. *Artemisia* and *Ephedra*) and halophyte (e.g. Caryophyllaceae, Amaranthaceae–Chenopodiaceae) elements ratio, and deciduous *Quercus* variations through the IM-5 agosto section (modified after Joannin, 2007).

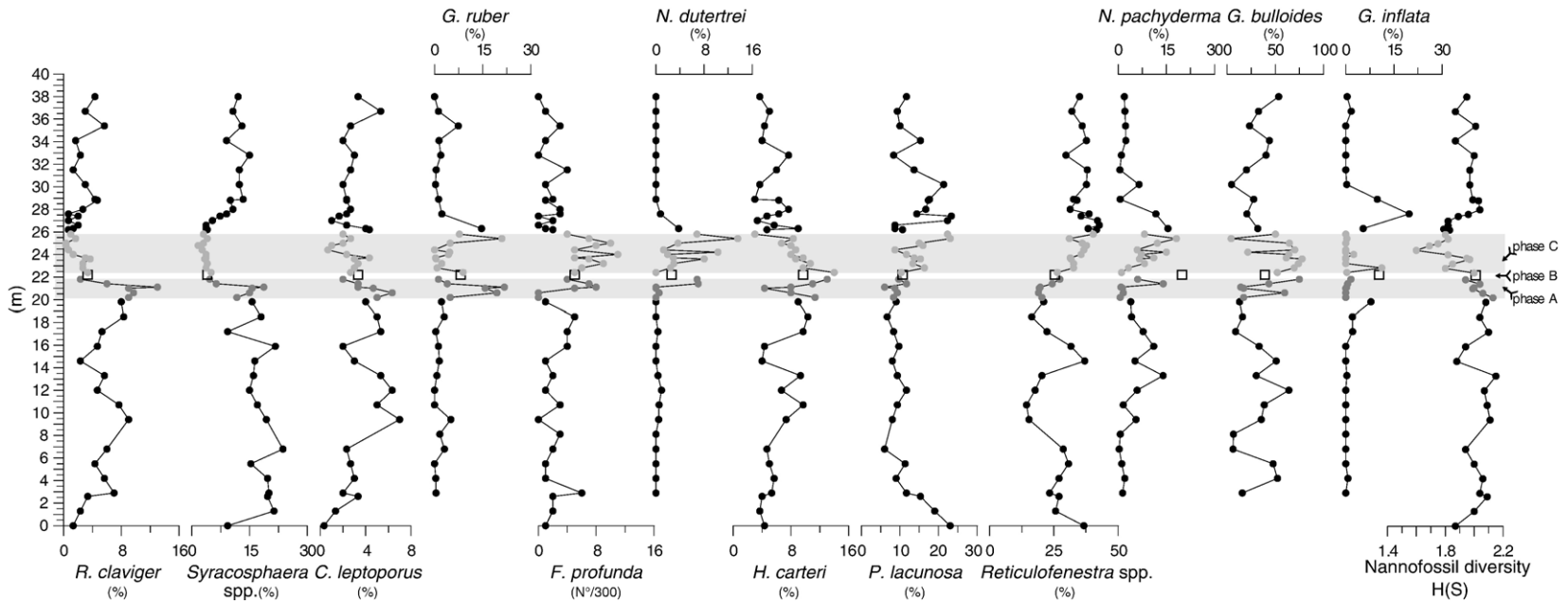


Fig. 9. Abundance patterns of selected calcareous nannofossils and planktonic foraminifera at the IM-5 agosto section. Planktonic foraminifera are from Stefanelli et al. (2005).

foraminifera (Stefanelli et al., 2005). In the pre- and post-sapropel sediments, the assemblage is well diversified and the most common taxa mainly consist of small placoliths, *Reticulofenestra* spp. (*R. asanoi*, *Reticulofenestra* sp. sensu Maiorano and Marino, 2004, and *R. minutula*), *Pseudoemiliana lacunosa*, *Coccolithus pelagicus*, *Syracosphaera* spp. (mainly *Syracosphaera histrica* and *S. pulchra*). Subordinate components in the assemblages are *Rhabdosphaera claviger*, *Calcidiscus leptoporus*, *Helicosphaera carteri*. Very rare and scattered taxa are represented by *Calciosolenia* spp., *Discosphaera tubifera*, *Pontosphaera* spp., *Umbilicosphaera* spp., *Braarudosphaera bigelowii*, *Helicosphaera* spp. Reworked species are common and almost uniformly distributed and generally represented by Cretaceous and Paleogene taxa.

The calcareous nannofossil assemblages show the most striking feature across the sapropel layer. The most evident aspects are represented by the increase in abundance of *F. profunda*, the decrease of *R. claviger* and *Syracosphaera* spp. and the increasing trend of *P. lacunosa* and *Reticulofenestra* spp. Specifically, during the lowermost part of phase A, *R. claviger*, *Syracosphaera* spp. and *C. leptoporus* are significant components of the nannofossil assemblages and show distinct peaks in abundance. Concomitant low abundances of *F. profunda*, *P. lacunosa* and *Reticulofenestra* spp. also characterize this interval. From the upper part of phase A through the whole sapropel layer, *R. claviger*, *Syracosphaera* spp. significantly decrease in abundance together with a slight decrease of *C. leptoporus*, although this taxon shows several short term abundance fluctuations. In the final stage of phase A, the beginning of an increasing trend of *Reticulofenestra* spp. and of *P. lacunosa* is observed. During the short interruption in the sapropel layer the calcareous nannofossil assemblages do not display distinctive features, with the exclusion of a slightly decrease in abundance of *F. profunda* and of *H. carteri*. However, *H. carteri* reaches maximum values slightly below and above phase B. An increase of *Reticulofenestra* spp. and *P. lacunosa* occurs through the whole phase C. In addition, *Reticulofenestra* spp. show important high values even slight above the top of the sapropel layer. Phase C is marked by a significant decreasing trend in the Shannon–Weaver index, with a minimum value occurring at 24.4 m.

### 3.3.3. Ostracods

A total number of 3477 valves have been recovered within the ostracod assemblages and 113 different species belonging to 51 genera have been identified.

Among these, due to the scattered or poorly preserved nature of the material, eighty species have been definitively or tentatively classified, thus leaving the remaining 33 ones in an open nomenclature.

Vertical distribution of all the species has been detected and only the most significant taxa considered for the discussion are reported in Fig. 10. All the most representative species occurring in the pre-sapropel interval are also present in the post-sapropel interval, with the only exception of *Cytheropteron testudo*, a well known Plio–Pleistocene northern guest (Aiello et al., 1996 and references therein) presently living in the North Atlantic Ocean.

The autochthonous assemblages in the IM-5 agosto section are dominated by genera (*Krithe*, *Cytheropteron*, *Henryhowella*, *Cytherella*, *Parakrithe*) commonly living in the Mediterranean waters both on the shelf and in the bathyal zone. Specifically, the distribution of autochthonous ostracod species at the IM-5 agosto section and its comparison with the paleobathymetric preferences of extant, Quaternary and Upper Pliocene Mediterranean assemblages indicate a paleodepth estimate of about 250–350 m (upper bathyal zone) as shown in Fig. 10.

The allochthonous valves range from 0 to 36.7/100 g and show a discontinuous trend through the IM-5 agosto section (Fig. 11). Paleoenvironmental changes were clearly observed by grouping *Krithe* and *Parakrithe* (K+P), *Cytheropteron* and *Henryhowella* (C+H) and by (K+P)/(C+H) ratio (Fig. 11). In the studied section the genera *Krithe* and *Parakrithe*, *Cytheropteron* and *Henryhowella* represent the most abundant infaunal and epifaunal taxa respectively. The mode of life of *Krithe* has been inferred from shell structure (e.g. Coles et al., 1994) and directly observed by Majoran and Agrenius (1995). *Parakrithe* shows very similar features and it is assumed as infaunal. *Henryhowella* is considered epifaunal on the basis of both the structure of the carapace and indirect observations (Kempf and Nink, 1993; Didié and Bauch, 2002). The genus *Cytheropteron* is characterized by more or less developed ventral expansions (alae) which are commonly interpreted as typical of taxa crawling over the bottom sediments (Elofson, 1941).

The lower part of the section, belonging to the whole pre-sapropel interval, up to the sample just above the onset of sapropel interval (0–20.2 m) is characterized by a high diversity of *Krithe* genus and by high K+P and C+H abundance (Fig. 11). Diversity indexes (Fig. 11) range from 1.24 to 2.62 (SH), from 0.67 to 0.90 (S1-D) and from 4 to 18 (SR). The (K+P)/(C+H), representing infaunal/epifaunal ratio, varies from 0.67 to 4.33

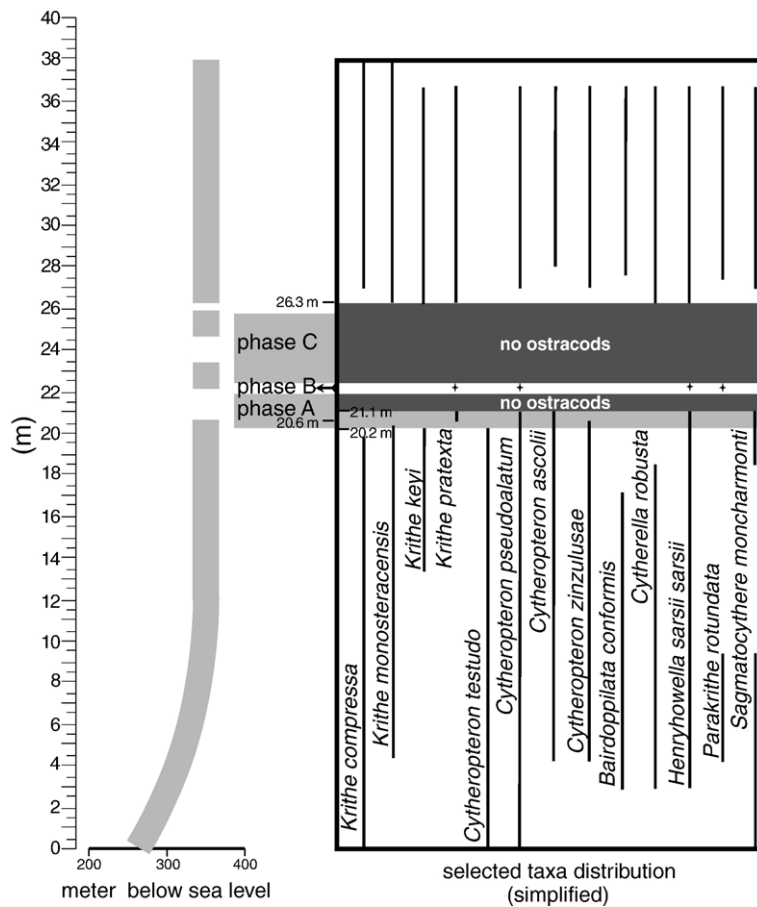


Fig. 10. Paleobathymetric variations through the IM-5 agosto section based on the ostracod assemblages, and stratigraphical distribution of selected taxa. Uncertainty in the paleodepth estimation is of some dozen metres.

(Fig. 11). The species *C. testudo* occurs exclusively in this part of the section. In addition, some species (e.g. *Bairdoppilata conformis*, *Cytherella robusta*) temporarily disappear (Fig. 10). In this part of the section the trend of diversity indexes has a positive relation with C+H abundance variations (Fig. 11). Conversely, K+P abundance and  $(K+P)/(C+H)$  follow a very clear inverse trend (Fig. 11).

In the lower part of phase A, infaunal ostracods become very rare: the species *Krithe pratexta* replaces *K. compressa*, *K. keyi* and *K. monosteracensis* (Fig. 10), with a collapse of K+P abundance (from 11.1 to 3.57%, Fig. 11). In contrast, C+H abundance (from 33.3 to 60.9%), mainly due to the abundance of the *Cytheropteron* genus, shows a marked increase (Fig. 11). Consequently, the infaunal/epifaunal ratio abruptly decreases (0.1–0.33). Abundance and diversity show opposite trends, the abundance being relatively low ( $OA_i=3.0-9.3$ ,  $OA_v=8.3-35.7$ ) and diversity high ( $SH=2.19-2.3$ ) (Fig. 11).

The interval ranging from the middle part of phase A up to the top of the sapropel interval is virtually barren (i.e. devoid of autochthonous ostracods), with the notable exception of an assemblage recovered in phase B largely dominated by *Henryhowella sarsii sarsii* and *K. pratexta* (Fig. 10). The barren interval extends up to 26.2 m (slightly above phase C), i.e. up to the level where the repopulation of benthic foraminifera (Stefanelli et al., 2005) had been already started.

The post-sapropel interval starts with the sudden return of ostracod fauna almost completely consisting of *H. sarsii sarsii* and the genus *Krithe*. This interval is characterized by the increase in abundance and regular occurrence of *B. conformis*, *C. robusta*, *Parakrithe rotundata* and *Sagmatocythere moncharmonti*. A distinct opposite trend of diversity indexes (especially S1-D) with K+P abundance and infaunal–epifaunal ratio is re-established, as in the pre-sapropel interval (Fig. 11). However, while in the pre-sapropel interval abundance and diversity are strictly related, in the post-sapropel

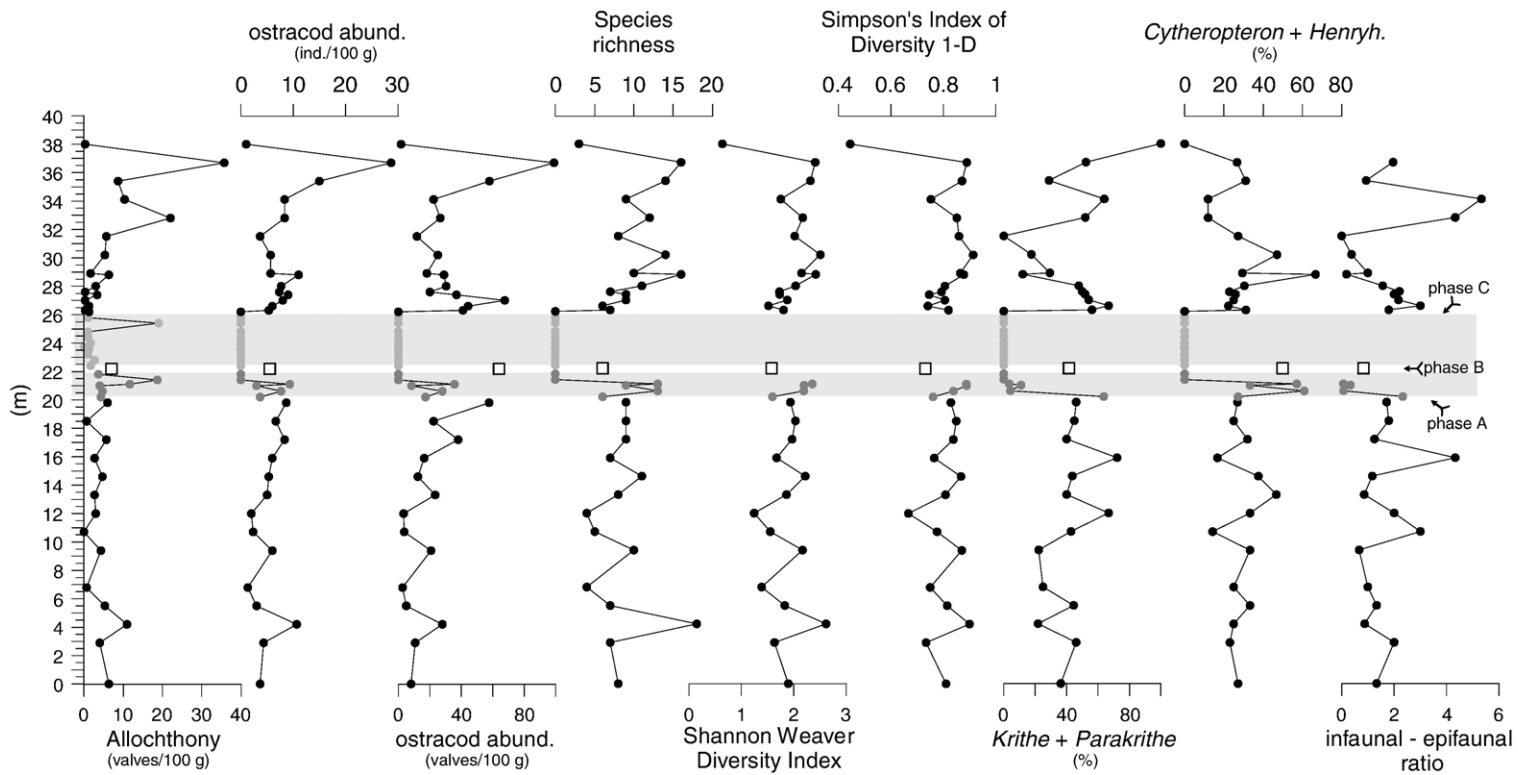


Fig. 11. Abundance variations of selected indexes in the ostracod assemblages at the IM-5 agosto section.

sediments no clear connection can be observed. In the uppermost part of the section Ostracod Abundance ( $OA_1$  and  $OA_v$ ) gradually reach the higher values (28.7/100 g and 99/100 g, respectively) of the whole section (Fig. 11).

## 4. Discussion

### 4.1. On-land paleoclimate conditions: terrigenous vs eolian input

The beginning of sapropel deposition is clearly marked by an evident increase in terrigenous input mainly characterized by clay minerals (sharp increase in  $Al_2O_3$  content and high clay minerals/quartz ratio; Figs. 5, 7). Specifically, a sharp increase of chlorite with respect to kaolinite is a distinctive feature of the sapropel deposition. In the sediments from the frontal part of the southern Apennines chain – which represents the source area of the Pleistocene sediments of the IM-5 agosto section (Casnedi, 1988) – as deduced from present-day marine sediments, the Kaol/Chl ratio ranges from 0.8 to 0.5 (Di Leo, unpublished data), very close to that observed in the sapropel sediments. This pattern can therefore be considered as a feature inherited from the source area, and it clearly suggests an increase in sediments load during sapropel deposition.

Using the elements/aluminum ratios of major and trace elements, including REE (see Appendix A), as variables in the input matrix of a multivariate statistical analysis using Principal Component Analysis (PCA) method (Fig. 12a), it can be observed that the first component (58% variance) groups together Ti/Al, Zr/Al, Si/Al, Si/Ti, and biogenic silica with high positive component loadings, and Ti/Zr with a negative component loading. The second component (30% variance), groups together La/Al, Ce/Al, La/Sc showing high positive component loadings, and V/Al with a negative component loading. In the 1st component vs. 2nd component plot, samples from sapropel interval group together in the direction of maximum variation of light rare earth elements (high La/Al, Ce/Al and low La/Sc c. loadings on the 2nd component), being enriched in light REE and depleted in Sc, and of maximum variation in Ti/Zr ratio (high c. loading on the 1st component).

In the 1st component vs 2nd component plot (Fig. 12a) sample from phase B falls in the direction of maximum variation of Ti/Al and Zr/Al ratio, suggesting a strong correlation between these variables which strongly enrich in this phase. It is well known that high immobile elements/Al ratios, i.e. Ti/Al, Zr/Al and low Ti/Zr ratios, indeed characterize eolian sediments: high Ti/Al ratio has been observed in eolian mineral particles from the Sahara–Sahel Dust Corridor (Moreno

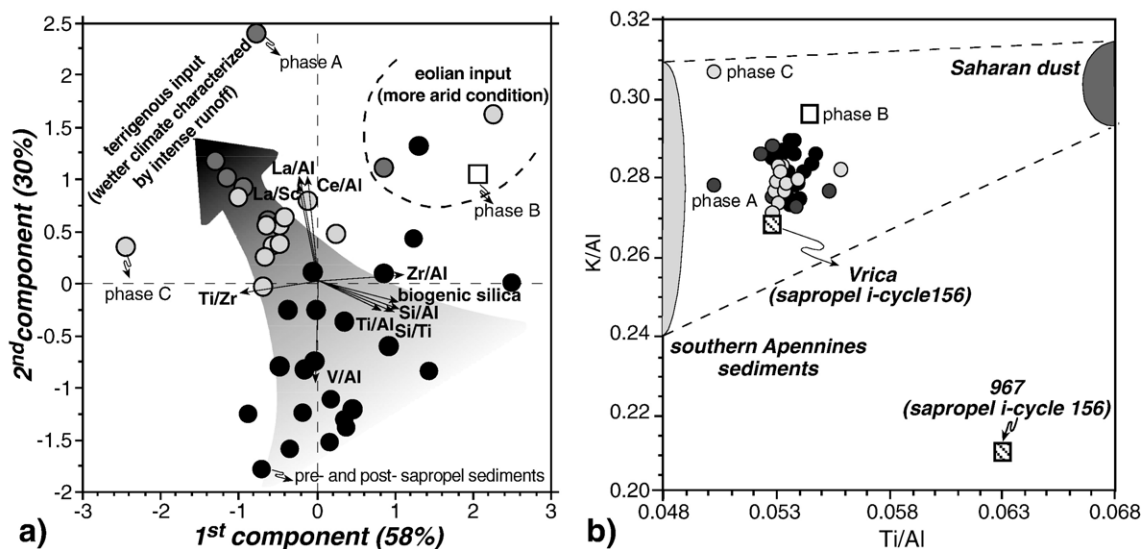


Fig. 12. a) Orthogonal plot of the multivariate statistical analysis carried out using Principal Component Analysis (PCA) as extraction method. In the input matrix weight ratios of chemical elements and the calculated biogenic silica (Robinson, 1994) from the IM-5 agosto section have been used. b) Plot of K/Al versus Ti/Al weight ratios. Sahara dust data from Krom et al. (1999b), southern Apennines data from Laviano (1991), Pescatore et al. (1980) and Di Leo et al. (2002). Data of the sapropel sediments from the Early Pleistocene i-cycle 156 of Vrica section and ODP Site 967 (Nijenhuis et al., 2001) are also included, the former as representative of an on-land section from bathyal setting, the latter of enhanced Nile river input.

et al., 2006). High Si/Al and Si/Ti ratios also characterize eolian sediments. On this basis, a significant eolian input may be invoked to explain the geochemical features of phase B. Ti/Al and K/Al are also specifically useful for distinguish between arid and humid condition, being these ratios high when a strong input from eolian (e.g. Sahara) dust occurs (Krom et al., 1999a,b). The relationship between K/Al and Ti/Al ratios (Fig. 12b) in fact, clearly indicate a significant eolian input from a Sahara source (Weldeab et al., 2002) for the sediments from the interruption (phase B). The 2nd component may represent the efficiency of fluvial erosion – which increased during sapropel deposition as consequence of paleoclimate changes (wetter climate characterized by intense freshwater runoff) – if one considers that the V is mainly associated with fine particles (Muller and Calas, 1987; Di Leo, 1998) and the REE are associated with minerals (e.g. feldspars, zircon, and phosphates) more represented in the silt fraction: sediments of sapropel interval are enriched in silt fraction (Fig. 4b) and are relatively enriched in feldspars (low Kaol/[Kfs+Pl] ratio; Fig. 7). The lower Kaol/Chl ratio observed in the sapropel further supports the hypothesis of increased runoff during sapropel deposition. Such intense terrigenous supply was not continuous in the sapropel interval: a reduction of the sediment flux occurred at about 22.2 m during the interruption of the sapropel (i.e. phase B). The interruption is enriched in kaolinite and feldspars with respect to quartz in sapropel and pre- and post-sediments. Comparison with data of atmospheric dust from Mediterranean areas (Tomadin and Lenaz, 1989; Prospero et al., 1981) suggests that the mineralogical signal may be consequence of an appreciable input from eolian dust. North African sediments are also characterized by large amount of kaolinite and feldspars (Moreno et al., 2006). However, marine transport of these sediments to Ionian Basin coast is unlikely because of the strong surface current flowing through the Siculo–Tunisian strait from the northwest to the southeast, acting as a hydrodynamic barrier (Mélières et al., 1998).

Despite a lower sampling resolution, pollen data-set further improve the on-land paleoclimate framework through the sapropel layer. Specifically, the beginning of phase A (Fig. 8) is marked by a strong increase of the mesothermic vs. steppic and halophyte ratio thus indicating warm and wet climate conditions. Phase B clearly records a return to cold and arid conditions. Italian coasts could receive less than 650 mm of annual precipitations or long seasonal summer dryness, which are the limiting factor for the deciduous *Quercus* development (Rossignol-Strick and Paterne, 1999).

Through phase C the mesothermic vs. steppic and halophyte ratio increases again reaching higher values only in the upper part of the interval, which suggests changing to warm and wet conditions.

#### 4.2. Sea surface water temperature, productivity and turbidity

Sea surface water temperatures have been reconstructed by means of calcareous nannofossils and planktonic foraminifera distributions (Stefanelli et al., 2005), together with some geochemical proxy. A multivariate statistical analysis using a PCA method (Fig. 13) has been performed using calcareous nannofossil abundance variations as variables in the input matrix together with the  $Al_2O_3$  content and the Kaol/Chl ratio as tracers for the terrigenous input – which may have significantly affected surface water phytoplankton community in such a proximal setting – and the U/Al ratio as a proxy of surface productivity combined with low oxygen bottom waters. A combination of anoxic bottom environment with high productivity in aerated surface waters is supposed to be the most favorable factor for uranium concentration in sedimentary process (Kochenov and Baturin, 2002).

The first component (43% variance) groups together *R. claviger*, *C. leptoporus* and *Syracosphaera* spp. with high positive component loadings, and *Reticulofenestra*

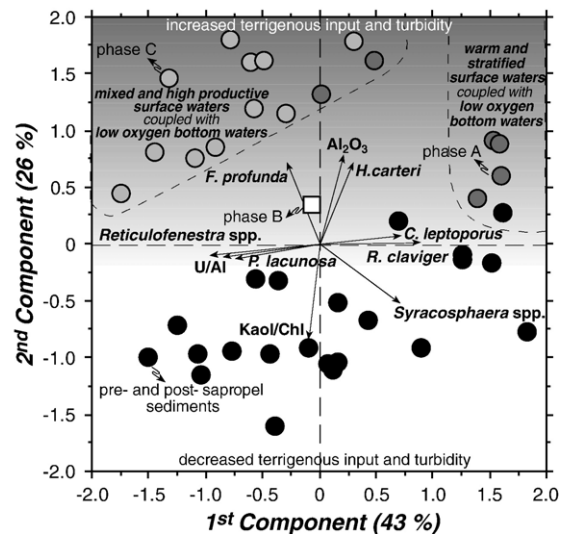


Fig. 13. Orthogonal plot of the multivariate statistical analysis carried out using Principal Component Analysis (PCA) as extraction method. In the input matrix both calcareous nannofossil abundances and geochemical variables from the IM-5 agostio section have been used.

spp. and *P. lacunosa* with negative component loadings. *R. claviger* and *Syracosphaera* spp. are upper photic zone taxa preferring warm and low nutrient environments (McIntyre et al., 1972; Roth and Coulbourn, 1982; Ziveri et al., 2004, among others). *C. leptoporus* seems to prefer tropical to subtropical oligotrophic, warm-water masses of upper and middle photic zones (McIntyre and Bé, 1967; McIntyre et al., 1970; Flores et al., 1999; Ziveri et al., 2004 among others). On the other hand, the ecology of the extinct species *P. lacunosa* and of the Pleistocene reticulofenestrids is not well known. However, they belong to placolith-bearing taxa that dominate the coastal and upwelling areas in the modern assemblages (Young, 1994). Therefore the ecological affinity among the taxa lumped in both the groups seems to indicate that the abundance patterns of calcareous nannofossils can be considered the result of an ecological response rather than a dissolution effect. Thus, the 1st component seems to discriminate between warm, oligotrophic and stratified surface water conditions, characterizing both the onset of oxygen depletion at the sea bottom and most of phase A, and high productive surface water conditions occurring in the uppermost part of phase A and in phase C. The decrease in diversity of calcareous nannofossils recorded during phase C, combined with the increase of eutrophic taxa (*Reticulofenestra* spp. and *P. lacunosa*) confirms such an interpretation and can be related to r-selected life strategies in eutrophic conditions (Young, 1994). Oligotrophic and warm surface water environments in the lower part of phase A are also recorded from the planktonic foraminiferal assemblages based on the increase in abundance of *Globigerinoides ruber* gr. and of high SST values (Figs. 2, 9). During the upper part of phase A and during phase C, high abundances of *G. bulloides*, *Neogloboquadrina pachyderma*, *N. dutertrei* in the planktonic foraminifera microfauna (Fig. 9) suggest an eutrophic environment with possible decrease in the year-round thermocline/halocline (Stefanelli et al., 2005). The relation of high U/Al ratio with *Reticulofenestra* spp., *P. lacunosa* in phase C (Fig. 13) supports the hypothesis of increased productivity coupled with low oxygen bottom water conditions as documented by Kochenov and Baturin (2002) specifically for anoxic environments. The second component (26% variance) sets apart pre-and post-sapropel sediments from those of the sapropel interval, lumping together, in the direction of maximum variation of Al<sub>2</sub>O<sub>3</sub> (high terrigenous content), *H. carteri* and *F. profunda*. *H. carteri* is known to be a coastal taxon and a marker of moderately elevated nutrient conditions and turbidity (Giraudeau, 1992; Ziveri et al., 1995; Ziveri

et al., 2000; Colmenero-Hidalgo et al., 2004). Thus, its positive relation with high Al<sub>2</sub>O<sub>3</sub> content in the sapropel interval is likely related to the high detrital and nutrient input as well as high turbidity of surface waters. On the other hand, the ecology of *F. profunda*, which is a deep-photic zone taxon, is not so clearly understood. It is well known that the light requirements of this taxon are much lower than those of most coccolithophores (Okada and Honjo, 1973; Brand, 1994; Cortés et al., 2001). However, the high abundance of the species has been often related to a Deep Chlorophyll Maximum (DCM) development (Rohling and Gieskes, 1989; Molino and McIntyre, 1990; Castradori, 1993). The present results seem to highlight an opportunistic behaviour of *F. profunda* likely related to low light surface water conditions (high turbidity) and low competition within the nanoplankton community. High abundances of *F. profunda* through most of the sapropel interval and particularly during phase C are, in fact, coupled with a reduced calcareous nannofossil diversity and increase of r-selected taxa. It is worthy to note that an upward migration of the species as a consequence of light decrease has been inferred by previous authors (Colmenero-Hidalgo et al., 2004). Although *F. profunda* significantly increases within the sapropel, the hypothesis of DCM development seems not well supported from the present results. The very low abundance of the oligotrophic taxa inhabiting the upper–middle photic zone (*R. claviger*, *C. leptoporus* and *Syracosphaera* spp.) appears in fact not in agreement with the occurrence of nutrient-rich deep photic layer combined with oligotrophic and stratified surface waters. Thus, the 2nd component may represent the turbidity of surface waters, which increases during sapropel deposition as consequence of higher detrital input associated to the increased freshwater runoff. The good correlation existing within the sapropel between *F. profunda* and *N. dutertrei* abundance patterns is also interesting (Fig. 9). The latter has been observed in reduced-salinity lenses associated to the sapropel deposition in particular during cooler phases (Vergnaud-Grazzini et al., 1977; Capotondi et al., 2000) and considered as a low salinity indicator (Cita et al., 1977), which is in good agreement with the increased fresh-water runoff.

Interruption of sapropel layer is not marked by major shifts in nannofossil assemblages. However, we observe a weak decrease of *F. profunda* and of *H. carteri* (Fig. 9) across phase B probably due to the decreased terrigenous input. In the same interval, planktonic foraminifera patterns show the re-occurrence of *Globorotalia inflata* and low percentages of *G. ruber* gr. (Fig. 9), suggesting vertical mixing of the water column with a breakdown

of the thermocline during cool climate conditions or increased seasonal contrast.

#### 4.3. Oxygen bottom water conditions

Changes in oxygen content during deposition of sapropel 19 at the IM-5 agosto section was recently investigated by the benthic foraminifera analyses (Stefanelli et al., 2005). In the present paper we used Ostracod abundance patterns as an additional proxy of the oxygen levels at the sea-floor. The high sensitiveness of Ostracoda to dissolved oxygen values has been highlighted in a number of papers (Peypouquet, 1977; McKenzie et al., 1989; Whatley, 1991; Whatley and Zhao, 1993; van Harten, 1995; Corbari, 2004), although a general consensus has not been yet achieved. On the other hand, it is generally accepted that, in a context of bathyal “low oxygen” sediments, abundance and diversity are largely dependent upon oxygen levels. Ostracod assemblages are very poor and scarcely diversified when  $O_2$  is  $<3$  ml/l (Peypouquet, 1977). During sapropel events ostracods are not able to survive in “anoxic” (*sensu* van Harten, 1987) environments.

In the pre-sapropel interval of the IM-5 agosto section ostracod diversity and abundance have a positive relation with epifaunal genera (C+H), and a negative one with infaunal (K+P) abundance (Fig. 11). This evidence suggests that the relationship between infaunal–epifaunal ostracod ratio and diversity can be tentatively proposed as indicative of changes in the oxygen content at the sea bottom as already shown in the same section on the base of the benthic foraminifera behaviour (Stefanelli, 2004 and references therein). Consequently a dissolved oxygen curve indicating aerobic and kenoxic (Cepek and Kemper, 1981; Whatley, 1990) phases is here proposed (Fig. 14). The aerobic phase is mainly characterized by high diversity and abundance and low values of infaunal–epifaunal ratio (Fig. 11); the kenoxic phase is recognized by relatively low diversity and abundance values and high infaunal–epifaunal ratio; the “no ostracod” interval is devoid of autochthonous remains (Fig. 11).

During the pre-sapropel interval, a slightly kenoxic/slightly aerobic environment dominates (Fig. 14), with a prevalence of oxic peaks in the lower part (0–12 m) and of kenoxic peaks in the upper part (12–20.2 m). The latter may represent the prelude to the gradual deterioration of the bottom paleoenvironment. In the lower part of phase A, the reversal trend between abundance and diversity, the disappearance of the previously recorded infaunal *Krithe* genus (Fig. 10) and the occurrence of the opportunistic species *K.*

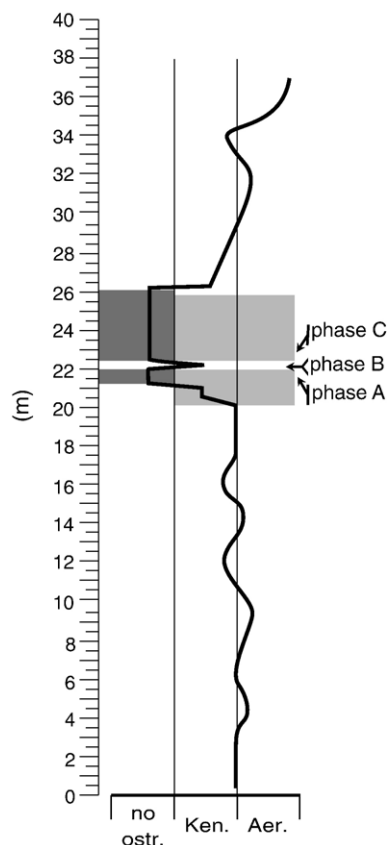


Fig. 14. Inferred oxygen bottom water variations based on changes in the ostracod assemblage. Ken.: kenoxic, Aer.: aerobic.

*praetexta* suggest that the balance of a slightly kenoxic/slightly aerobic environment is lost. This interval has been interpreted as a kenoxic phase (Fig. 14) (i.e. “upper dysaerobic” *sensu* Stefanelli et al., 2005). The genus *Cytheropteron* dominates and the infaunal–epifaunal ratio drops from 0.33 to 0.06. Therefore, it is clear that a limiting parameter in ostracod infaunal distribution occurs, and this is likely related to the rising of the redox front through the sediment pore-waters due to the decreased oxygen content at the sea bottom.

The next step, characterized by the complete loss of ostracods at the top of phase A, suggests the occurrence of very low oxygen content even at the sediment–water interface. Comparison between ostracod and benthic foraminifera patterns suggests that some benthic specimens, which do not completely disappear within the sapropel, tolerate lower values of dissolved oxygen, and an “ostracod anoxic event” may be the equivalent of a “foraminifer dysoxic event”.

A short-term amelioration in the oxygen content occurs during phase B, with a return to kenoxic conditions. The occurrence of *K. praetexta* in this interval (Fig. 10) confirms that the species is able to tolerate low oxygen conditions and suggests adaptation of the taxon to rapid and short-term paleoenvironmental changes. The restoring of kenoxic conditions is quick. In the post-sapropel interval the assemblage diversity gradually increases (Fig. 11), while the infaunal–epifaunal ratio and the K+P abundance decrease, indicating a progressive recolonization likely linked to the transition from kenoxic to aerobic paleoenvironment (Fig. 14).

Above 31.5 m, the diversity and the K+P and infaunal–epifaunal ratio trends document a new shift towards kenoxic conditions, with a trough in oxygen curve at 34.1 m. The peaks in diversity, abundance and species richness and low values of infaunal–epifaunal ratio from 35.4 to 36.7 m interval indicate improved oxygenation of the bottom water (Figs. 11, 14).

The ostracod assemblages suggest that the oxygen content at the sea bottom was significantly reduced during sapropel deposition, supporting the previous reconstruction based on benthic foraminifera (Stefanelli et al., 2005). However, ostracod assemblages suggest that the oxygen content at the sea bottom was also significantly diminished just above phase C (Fig. 14). This slightly different responses with respect to previous data (Stefanelli et al., 2005) is likely related to the different efficiency of foraminifera and ostracoda to oxygen depletion at the bottom sediment. The data in Fig. 2 support the hypothesis that the benthic foraminifera are the more tolerant meiofaunal group with respect to the oxygen content (Moodley et al., 1997).

## 5. Depositional constraints of sapropel 19

The formation of sapropel 19 (i-cycle 90) occurred during a warm climatic conditions correlated to MIS 25. With the exception of the interruption, most of the geochemical and mineralogical proxies strongly support the hypothesis that the sapropel deposition is likely related to an enhanced freshwater runoff induced by a wetter climate and stronger monsoon in the eastern Mediterranean region (Rossignol-Strick, 1983; Wehausen and Brumsack, 2000). As a consequence, a more efficient fluvial erosion was promoted causing an increase of terrigenous input. In such a proximal setting increased turbidity occurred in surface waters. A clear paleoenvironmental variability characterizes the sapropel 19 deposition, and the inferred paleoenvironmental

features are summarized in a final sketch (Fig. 15). Specifically, during the lower part of phase A, a strong increase of wetness on land, associated with warmer palaeoclimate conditions is attested by the higher abundances of mesothermic pollen taxa. At the same time, in the marine environment, the oxygen content starts to decrease at the sea floor, as testified by the first significant change in the benthic foraminifera realm (Stefanelli et al., 2005) and, slightly after, in the ostracod assemblages, as suggested by the significant reduction of the infaunal abundance and by the occurrence of the opportunistic taxon *K. praetexta*. In this interval, high diversity in the calcareous nannoplankton assemblage and high abundance of *Syracosphaera* spp., *R. claviger* and *C. leptoporus* document warm and oligotrophic conditions in the upper water column at the beginning of sapropel deposition, in agreement with Sea Surface Temperature (SST) curve based on planktonic foraminifera (Fig. 2). Warm and humid climate conditions responsible for the enhanced run-off and consequent increase of higher fresh water input seem to have triggered the onset of sapropel deposition (Fig. 15). During the upper part of phase A, the relative increase of the Ti/Al ratio suggests increment of the eolian input (i.e. a gradual changes to more arid conditions). Surface water proxies (increase of *Reticulofenestra* spp., *G. bulloides* and *N. pachyderma* and decrease of *R. claviger*, *Syracosphaera* spp. and *G. ruber*) suggest a cooler and moderately productive environment. The concomitant enhanced depletion of the oxygen content at the sea floor, as evidenced by the beginning of the ostracod-barren interval, may be an indication of an increased input of organic matter to the sea floor and relative increase of oxygen consumption (Fig. 15). Temporary re-population of benthic foraminifera and ostracod fauna underline a sudden re-oxygenation of the sediment (phase B). Pollen data document cool and arid conditions on land. Sea surface temperature based on planktonic foraminifera indicates cool climate conditions as well (Fig. 2). According to the geochemical and mineralogical indexes, arid conditions started in the upper part of phase A and culminates during phase B. In particular, the high CM/Qz, Kaol/Qz, Kaol/Chl joined to the high Ti/Al and K/Al ratios recorded in phase B indicate a river supply reduction and an eolian input increase (Sahara dust). These data suggest that the sapropel interruption can be related to intensified windblown activity and climate cooling, which probably ensured enhanced surface water density and convection of water column. This mechanism was most probably responsible for the improved bottom water ventilation. Similarly to what supposed for the Holocene sapropel

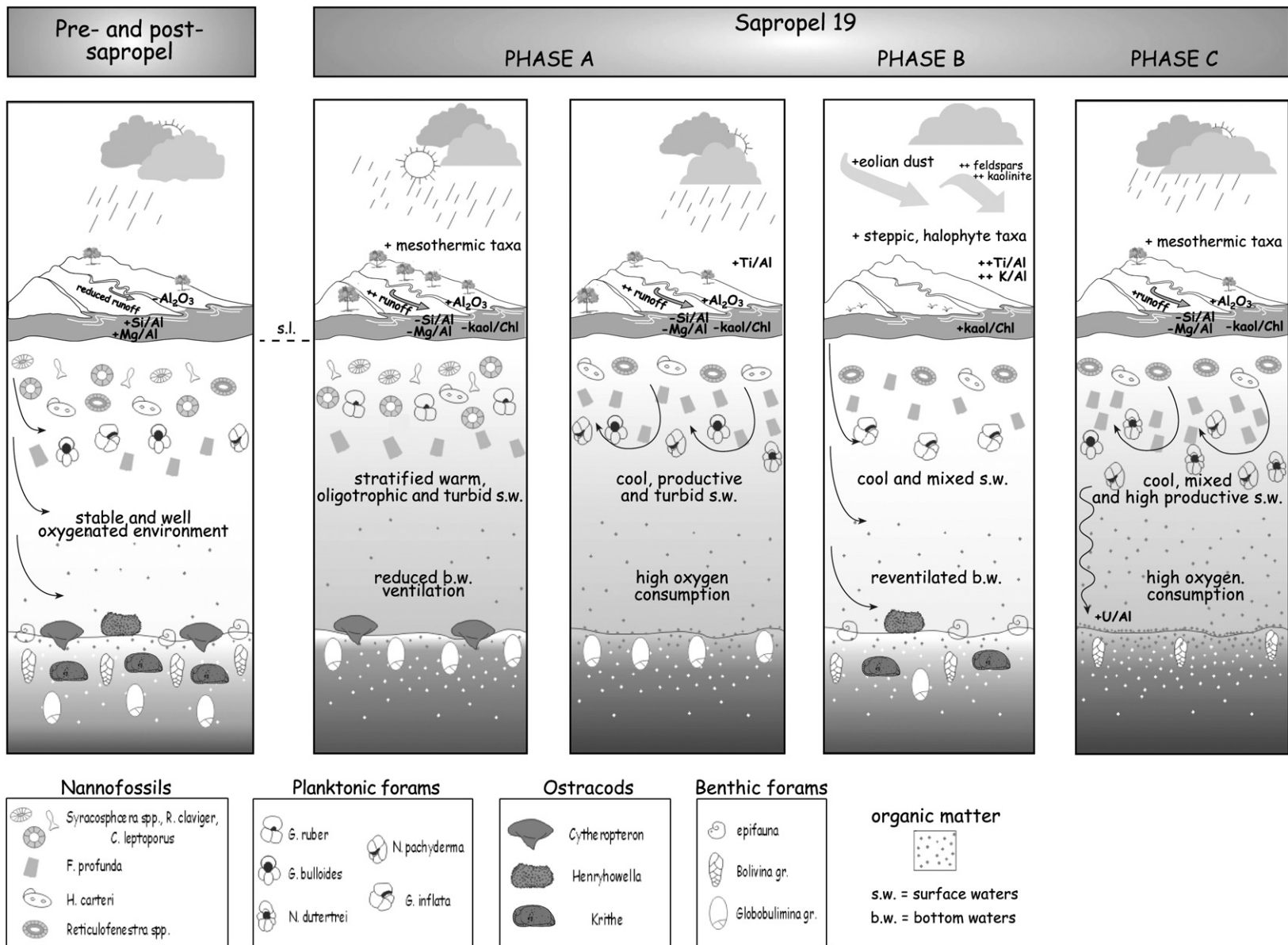


Fig. 15. Inferred paleoenvironmental features occurring during sapropel 19 deposition and in the pre-and post sapropel interval at the IM/5 agosto section.

S1 (De Rijk et al., 1999; Myers and Rohling, 2000), the sapropel interruption recorded at the IM-5 agosto section appears associated to a cooling and arid event. During such a period, the detrital river supply to the sea would have significantly decreased, increasing the relative concentration of wind-transported material from an African source in the sediments. Furthermore, during the interruption of sapropel 19, biogenic silica, which can be related to enhanced diatom productivity, increases. This observation may support the hypothesis that enhanced atmospheric dust, during the more arid and colder interval, was responsible for increased fertility in the surface waters (Harrison, 2000). Since a detailed diatom distribution is not available at the IM-5 agosto section, an eolian input for the biogenic silica cannot be excluded. Freshwater *Aulacoseira* diatoms, commonly combined with clay to form rounded clay-diatom agglomerations constitute, together with kaolinite, the main component of the Bodélé Depression sediments in Chad (north Africa), the world's largest natural source of silicate dust resulting from desiccated diatomaceous lake deposits (Moreno et al., 2006).

The rapid restoration of oxygen depleted conditions at the beginning of phase C is indicated by the reoccurrence of barren ostracod sediments and decrease in benthic foraminifera diversity. This phase is associated also to a quick re-establishment of humid conditions (Fig. 15), evidenced by abrupt mineralogical and geochemical changes. However, mesothermic taxa and SST records indicate that cool conditions still persisted at initial stage of phase C and only gradually changed toward warmer conditions up to the end of phase C. An increase in calcareous plankton productivity of surface waters can be hypothesized during phase C, on the basis of a continuous increment of *Reticulofenestra* spp. and *P. lacunosa*, a decrease in nannofossil diversity and high abundances of *G. bulloides* and *N. pachyderma*. During phase C, productivity may have been sustained by both the mixing of the deep layer and by the restored increased runoff (local riverine input). The rarity of oligotrophic taxa (*Syracosphaera* spp., *R. claviger*) and the increase of U/Al ratio underline the high surface water productivity.

The end of warmer and wetter paleoclimatic conditions at the top of phase C is clearly marked by the sharp variation of the geochemical and mineralogical parameters and a concomitant increase in calcareous nannoplankton diversity, likely favoured by a restored "normal" run-off, turbidity and nutrient availability in surface waters. However, according to the ostracod behaviour, it seems that the low oxygen conditions at the sea bottom, slightly persisted still above the re-

establishment of diverse benthic foraminifera assemblages at the end of phase C. A persistent low oxygen condition coupled with high productive surface waters slightly above the phase C is supported by high abundance values of *Reticulofenestra* spp. and the high U/Al ratio.

## 6. Conclusions

The multiproxy approach based on geochemical, mineralogical, micropaleontological studies performed on the on-land IM-5 agosto section reveals the main abiotic and biotic signals recorded during the deposition of the interrupted sapropel 19, thus helping to better understand the mechanism of sapropel formation in a more shallow (upper bathyal) environmental setting.

The deposition of sapropel 19 appears to be the result of a strong interaction between climate, local riverine input and sea floor ventilation. Warm and humid conditions characterize the onset of sapropel deposition, associated with higher freshwater input and decrease in salinity. Although the environmental setting of the studied section was remote from the deep water influence during the deposition of sapropel 19, the present results indicate a connection between changes in surface water properties and oxygen content at the sea bottom, in agreement with most sapropel scenarios (Rohling, 1994, 2001; Emeis et al., 2003; Rohling et al., 2006). Our results confirm that considerable paleoenvironmental variations can occur during deposition of an individual sapropel layer.

Productivity appears not to be high at the beginning of the studied sapropel, therefore not supporting the hypothesis that enhanced productivity was the primary factor triggering sapropel deposition (De Lange and Ten Haven, 1983; Calvert, 1983; Pedersen and Calvert, 1990), similarly to what occurred at the beginning of late Pliocene sapropel "c" at Vrica section (Negri et al., 2003). However, an increase in productivity seems to have occurred in the remaining of the studied sapropel 19, likely caused by cooling and enhanced mixing of water column, although an increase in land-derived nutrients, as a consequence of the increased river supply, cannot be excluded in such a proximal setting. Low oxygen conditions persist at the sea bottom during the whole sapropel, with the exception of the short interruption, when short-term mixing of water column developed under cool and arid climate conditions. More specifically, the estimated duration of  $0.350 \pm 0.32$  kyr for the interruption of sapropel 19 in the IM-5 agosto section represents the expression of a climate deterioration during which a significant increase in eolian input from a Sahara source prevailed over river supply.

## Acknowledgments

Two anonymous reviewers are greatly acknowledged for cooperative comments and corrections on the original version of the manuscript. This paper was financially supported by “Fondi Ateneo” 2005 granted to Prof. N. Ciaranfi. Chemical and mineralogical analyses were funded by the Italian Ministry of University and Research PRIN 2005 (Prof. M. Schiattarella) funds.

## Appendix A. Supplementary data

Supplementary data associated with this article can be found, in the online version, at [doi:10.1016/j.palaeo.2007.10.025](https://doi.org/10.1016/j.palaeo.2007.10.025).

## References

- Aiello, G., Barra, D., Bonaduce, G., 1996. The genus *Cytheropteron* Sars, 1866 (Crustacea: Ostracoda) in the Pliocene–Early Pleistocene of the M. San Nicola Section (Gela, Sicily). *Micropaleontology* 42 (2), 167–178.
- Arnaboldi, M., Meyers, P.A., 2003. Geochemical evidence for paleoclimatic variations during deposition of two Late Pliocene sapropels from the Vrica section, Calabria. *Palaeogeogr. Palaeoclimatol. Palaeoecol.* 190, 257–271.
- Beaudouin, C., Suc, J.-P., Escarguel, G., Arnaud, M., Charmasson, S., 2007. The significance of pollen record from marine terrigenous sediments: the present-day example of the Gulf of Lions (Northwestern Mediterranean Sea). *Geobios* 40, 159–172.
- Bown, P.R., Young, J.R., 1998. Chapter 2: techniques. In: Bown, P.R. (Ed.), *Calcareous Nannofossil Biostratigraphy*. Kluwer Academic Publishing, Dordrecht, pp. 16–28.
- Brand, L.E., 1994. Physiological ecology of marine coccolithophores. In: Winter, A., Siesser, W. (Eds.), *Coccolithophores*. Cambridge University Press, Cambridge, pp. 39–49.
- Brouwers, E.M., 1988. Sediment transport detected from analysis of ostracod population structure: an example from the Alaska continental shelf. *Ostracoda in the Earth Sciences*. Elsevier, Amsterdam, pp. 231–244.
- Calvert, S.E., 1983. Geochemistry of Pleistocene sapropels and associated sediments from the eastern Mediterranean. *Oceanol. Acta* 6, 225–267.
- Capotondi, L., Morigi, C., Turi, B., Brilli, M., 2000. Biological and oxygen isotope records in Late Quaternary sediments from the Eastern Mediterranean Sea, vol. 134. *Istituto Lombardo, Accademia di Scienze e Lettere, Milano*, pp. 169–183.
- Casnedi, R., 1988. La Fossa bradanica: origine, sedimentazione e migrazione. *Mem. Soc. Geol. Ital.* 41, 439–448.
- Casford, J.S.L., Abu-Zied, R., Rohling, E.J., Cooke, S., Boessenkool, K.P., Brinkhuis, H., DeVries, C., Wefer, G., Geraga, M., Papatheodorou, G., Croudace, I., Thomson, J., Lykousis, V., 2001. Mediterranean climate variability during the Holocene. *Mediterr. Mar. Sci.* 2, 45–55.
- Casford, J.S.L., Rohling, E.J., Abu-Zied, R.H., Fontanier, C., Jorissen, F.J., Leng, M.J., Schmiedl, G., Thomson, J., 2003. A dynamic concept for eastern Mediterranean circulation and oxygenation during sapropel formation. *Palaeogeogr. Palaeoclimatol. Palaeoecol.* 190, 103–119.
- Castradori, D., 1993. Calcareous nannofossils and the origin of eastern Mediterranean sapropel. *Paleoceanography* 8 (4), 459–471.
- Cepek, W.A., Kemper, E., 1981. Der Blättertonstein des nordwestdeutschen Barrême und die Bedeutung des Nannoplanktons für die fein laminiereten, anoxisch entstandenen Gesteine. *Geol. Jahrb., Hannover* A58, 3–13.
- Ciaranfi, N., D’Alessandro, A., 2005. Overview of the Montalbano Jonico area and section: a proposal for a boundary stratotype for the lower–middle Pleistocene, Southern Italy Foredeep. *Quat. Int.* 131, 5–10.
- Ciaranfi, N., D’Alessandro, A., Girone, A., Maiorano, P., Marino, M., Soldani, D., Stefanelli, S., 2001. Pleistocene sections in the Montalbano Jonico area and the potential GSSP for Early–Middle Pleistocene in the Lucania Basin (Southern Italy). *Mem. Sci. Geol.* 53, 67–83.
- Cita, M.B., Vergnaud-Grazzini, C., Robert, C., Chamley, H., Ciaranfi, N., D’Onofrio, S., 1977. Paleoclimatic record of a long deep sea core from the eastern Mediterranean. *Quat. Res.* 8, 205–235.
- Cita, M.B., Beghi, C., Camerlenghi, A., Kastens, K.A., McKoy, F.W., Nosetto, A., Parisi, E., Scolari, F., Tomadin, L., 1984. Turbidites and megaturbidites from the Herodotus abyssal plain (Eastern Mediterranean) unrelated to seismic events. *Mar. Geol.* 55, 79–101.
- Coles, G.P., Whatley, R.C., Mokuilevsky, A., 1994. The ostracod genus *Krithe* from the Tertiary and Quaternary of the North Atlantic. *Paleontology* 37 (1), 71–120.
- Colmenero-Hidalgo, E., Flores, J.A., Sierro, F.J., Bárcena, M.Á., Löwemark, L., Schönfeld, J., Grimalt, J.O., 2004. Ocean surface water response to short-term climate changes revealed by coccolithophores from the Gulf of Cadiz (NE Atlantic) and Alboran Sea (W Mediterranean). *Palaeogeogr. Palaeoclimatol. Palaeoecol.* 205, 317–336.
- Combourieu-Nebout, N., 1987. Les premiers cycles glaciaire–interglaciaire en région méditerranéenne d’après l’analyse palynologique de la série plio–pléistocène de Crotone (Italie méridionale). PhD Thesis, University Montpellier 2, France.
- Corbari, L., 2004. Physiologie respiratoire, comportementale et morphofonctionnelle des ostracodes Podocopes et Mydocopes et d’un amphipode caprellidé profond. Stratégies adaptatives et implications évolutives. Thesis, Université Bordeaux 1, France.
- Cortés, M.Y., Bollmann, J., Tierstein, H.R., 2001. Coccolithophore ecology at the HOT station, Hawaii. *Deep-Sea Res.* II 48, 1957–1981.
- Cour, P., 1974. Nouvelles techniques de détection des flux et de retombées polliniques : étude de la sédimentation des pollens et des spores à la surface du sol. *Pollen Spores* 16 (1), 103–141.
- D’Alessandro, A., La Perna, R., Ciaranfi, N., 2003. Response of macrobenthos to changes in palaeoenvironments in the Lower–Middle Pleistocene (Lucania Basin, Southern Italy). *Il Quaternario* 16, 167–182.
- De Lange, G.J., Ten Haven, H.L., 1983. Recent sapropel formation in the eastern Mediterranean. *Nature* 305, 797–798.
- De Rijk, S., Hayes, A., Rohling, E., 1999. Eastern Mediterranean sapropel S1 interruption: an expression of the onset of climatic deterioration around 7 ka BP. *Mar. Geol.* 153, 337–343.
- Didié, C., Bauch, H.A., 2002. Implications of upper Quaternary stable isotope records of marine ostracodes and benthic foraminifers for paleoecological and paleoceanographical investigations. In: Holmes, J. A., Chivas, A. (Eds.), *The Ostracoda: Applications in Quaternary research*. AGU Geophysical Monograph Series, vol. 131, pp. 279–299.
- Di Leo, P., 1998. I metalli pesanti nei sedimenti del Golfo di Manfredonia — Contaminazione antropica o processo naturale? *Miner. Petrogr. Acta* 41, 127–144.
- Di Leo, P., Dinelli, E., Mongelli, G., Schiattarella, M., 2002. Geology and geochemistry of Jurassic pelagic sediments, Scisti silicei Formation, southern Apennines, Italy. *Sediment. Geol.* 150, 229–246.

- Elofson, O., 1941. Zur Kenntnis der marinen Ostracoden Schwedens, mit besonderer Berücksichtigung des Skageraks: Uppsala Univ. Zool. Bidr. Upps. 19, 215–534.
- Emeis, K.-C., Schulz, H., Struck, U., Rossignol-Strick, M., Erlenkeuser, H., Howell, M.W., Kroon, D., Mackensen, A., Ishizuka, S., Oba, T., Sakamoto, T., Koizumi, I., 2003. Eastern Mediterranean surface water temperatures and  $\delta^{18}\text{O}$  composition during deposition of sapropels in the Late Quaternary. *Paleoceanography* 18. doi:10.1029/2000PA000617.
- Flores, J.A., Gersonde, R., Sierro, F.J., 1999. Pleistocene fluctuations in the Agulhas Current Retroflexion based on the calcareous plankton record. *Mar. Micropaleontol.* 37, 1–22.
- Folk, R.L., 1980. *Petrology of Sedimentary Rocks*. Hemphill's Bookstore, Austin. 182 pp.
- Giraudeau, J., 1992. Distribution of recent nannofossils beneath the Benguela system: Southwest African continental margin. *Mar. Geol.* 108, 219–237.
- Harrison, K.J., 2000. Role of increased marine silica input on paleo- $p\text{CO}_2$  levels. *Paleoceanography* 15 (3), 292–298.
- Hassold, N., Rea, D.K., Meyers, P.A., 2003. Grain size evidence for variations in delivery of terrigenous sediments to a Middle Pleistocene interrupted sapropel from ODP Site 969, Mediterranean Ridge. *Palaeogeogr. Palaeoclimatol. Palaeoecol.* 190, 211–219.
- Heusser, L.E., 1988. Pollen distribution in marine sediments on the continental margin off northern California. *Mar. Geol.* 80, 131–147.
- Hilgen, F.J., 1991. Astronomical calibration of Gauss to Matuyama sapropels in the Mediterranean and implication for the Geomagnetic Polarity Time Scale. *Earth Planet. Sci. Lett.* 104, 226–244.
- Hilgen, F.J., Krijgsman, W., Langereis, C.G., Lourens, L.J., 1997. Breakthrough made in dating of the geological record. *EOS, Trans.-Am. Geophys. Union* 78, 286–289.
- Howell, M.W., Thunell, R.C., 1992. Organic carbon accumulation in Bannock Basin: evaluating the role of productivity in the formation of eastern Mediterranean sapropels. *Mar. Geol.* 103, 461–471.
- Joannin, S., 2007. Changements climatiques en méditerranée à la transition Pléistocène inférieur-moyen: pollens, isotopes stables et cyclostratigraphie. PhD Thesis, University Lyon 1, France.
- Kempf, E.K., Nink, C., 1993. *Henryhowella asperrima* (Ostracoda) aus der Typusregion (Miozän: Badenian; Wiener Becken): *Sonderver. Geol. Inst. Univ. Köln* 70, 95–114.
- Kochenov, A.V., Baturin, G.N., 2002. The paragenesis of organic matter, phosphorus and uranium in marine sediments. *Lithol. Miner. Resour.* 37, 126–140.
- Krom, M.D., Cliff, R.A., Eijsink, L.M., Herut, B., Chester, R., 1999a. The characterization of Saharan dusts and Nile particulate matter in sediments from the Levantine basin using Sr isotopes. *Mar. Geol.* 155, 319–330.
- Krom, M.D., Michard, A., Cliff, R.A., Strohle, K., 1999b. Sources of sediment to the Ionian Sea and western Levantine basin of the Eastern Mediterranean during S-1 sapropel times. *Mar. Geol.* 160, 45–61.
- Laskar, J., Robutel, P., Joutel, F., Gastineau, M., Correia, A.C.M., Levrard, B., 2004. A long-term numerical solution for the insolation quantities of the Earth. *Astron. Astrophys.* 428, 261–285. doi:10.1051/0004-6361:20041335.
- Laviano, R., 1991. Nuovi dati mineralogici, chimici e granulometrici sulle argille plioceniche dell'area urbana di Potenza. *Geol. Appl. Idrogeol.* 26, 215–229.
- Lourens, L., 2004. Revised tuning of Ocean Drilling Program Site 964 and KC01B (Mediterranean) and implications for the  $\delta^{18}\text{O}$ , tephra, calcareous nannofossil, and geomagnetic reversal chronologies of the past 1.1 Myr. *Paleoceanography* 19 (3). doi:10.1029/2003PA000997.
- Lourens, L.J., Hilgen, F.J., Gudjonsson, L., Zachariasse, W.J., 1992. Late Pliocene to Early Pleistocene astronomically forced sea surface productivity and temperature variations in the Mediterranean. *Mar. Micropaleontol.* 19, 49–78.
- Lourens, L., Antonarakou, A., Hilgen, F.J., Van Hoof, A.A.M., Vergnaud Grazzini, C., Zachariasse, W.J., 1996. Evaluation of the Plio-Pleistocene astronomical timescale. *Paleoceanography* 11, 391–413.
- Maiorano, P., Marino, M., 2004. Calcareous nannofossil bioevents and environmental control on temporal and spatial patterns at the early-middle Pleistocene. *Mar. Micropaleontol.* 53, 405–422.
- Maiorano, P., Marino, M., Di Stefano, E., Ciaranfi, N., 2004. Calcareous nannofossil events in the lower-middle Pleistocene transition at the Montalbano Jonico section and ODP Site 964: calibration with isotope and sapropel stratigraphy. *Riv. Ital. Paleontol. Stratigr.* 110 (2), 547–557.
- Majoran, S., Agrenius, S., 1995. Preliminary observations on living *Krithe praetexta praetexta* (Sars, 1866), *Sarsicytheridea bradii* (Norman, 1865) and other marine ostracods in aquaria. *J. Micropalaeont.* 14, 96.
- Matsuoka, H., Okada, H., 1989. Quantitative analysis of Pleistocene nanнопланктон in the subtropical northwestern Pacific Ocean. *Mar. Micropaleontol.* 14, 97–118.
- McKenzie, K.G., Majoran, S., Emami, V., Reymont, R.A., 1989. The *Krithe* problem — first test of Peypouquet's hypothesis, with a redescription of *Krithe praetexta praetexta* (Crustacea, Ostracoda). *Palaeogeogr. Palaeoclimatol. Palaeoecol.* 74, 343–354.
- McIntyre, A., Bè, A.H.W., 1967. Modern coccolithophores of the Atlantic Ocean — I. Placolith and cyrtoliths. *Deep-Sea Res.* 14, 561–597.
- McIntyre, A., Bè, A.H.W., Roche, M.B., 1970. Modern Pacific Coccolithophorida: a paleontological thermometer. *Trans. N. Y. Acad. Sci. Trans. Ser II* 32, 720–731.
- McIntyre, A., Ruddiman, W.F., Jantzen, R., 1972. Southward penetrations of the North Atlantic Polar Front: faunal and floral evidence of large-scale surface water mass movements over the last 225,000 years. *Deep-Sea Res.* 19, 61–77.
- McManus, J., Berelson, W.M., Klinkhammer, G.P., Johnson, K.S., Coale, K.H., Anderson, R.F., Kumar, N., Burdige, D.J., Hammond, D.E., Brumsack, H.J., McCorkle, D.C., Rushdi, A., 1998. Geochemistry of barium in marine sediments: implications for its use as a paleoproxy. *Geochim. Cosmochim. Acta* 62, 3453–3473.
- Mélières, F., Foucault, A., Blanc-Valleron, M.-M., 1998. Mineralogical record of cyclic climate changes in Mediterranean Mid-Pliocene deposits from Hole 964A (Ionian Basin) and from Punta Piccola (Sicily). In: Robertson, A.H.F., Emeis, K.-C., Richter, C., Camerlenghi, A. (Eds.), *Proc. ODP Sci. Res.*, vol. 160. Ocean Drilling Program, College Station, TX, pp. 219–226.
- Mercene, D., Thomson, J., Abu-Zied, R.H., Croudace, I.W., Rohling, E.J., 2001. High-resolution geochemical and micropaleontological profiling of the most recent eastern Mediterranean sapropel. *Mar. Geol.* 177, 25–44.
- Meyers, P.A., Arnaboldi, M., 2005. Trans-Mediterranean comparison of geochemical paleoproductivity proxies in a mid-Pleistocene interrupted sapropel. *Palaeogeogr. Palaeoclimatol. Palaeoecol.* 222, 313–328.
- Meyers, P.A., Bernasconi, S.M., 2005. Carbon and nitrogen isotope excursions in mid-Pleistocene sapropels from the Tyrrhenian Basin: Evidence for climate-induced increases in microbial primary production. *Mar. Geol.* 220, 41–58.
- Molfino, B., McIntyre, A., 1990. Nutricline variation in the equatorial Atlantic coincident with the Younger Dryas. *Paleoceanography* 5, 997–1008.
- Moodley, L., Van der Zwaan, G.J., Herman, P.M.J., Kempers, A.J., van Breugel, P., 1997. Differential response of benthic meiofauna to

- anoxia with special reference to Foraminifera. Protista: Sarcodina. *Mar. Ecol., Prog. Ser.* 158, 151–163.
- Moreno, T., Querol, X., Castillo, S., Alastuey, A., Cuevas, E., Herrmann, L., Mounkaila, M., Elvira, J., Gibbons, W., 2006. Geochemical variations in aeolian mineral particles from the Sahara–Sahel Dust Corridor. *Chemosphere* 65, 261–270.
- Muller, J.P., Calas, G., 1987. Genetic significance of paramagnetic centers in kaolinites. In: Murray, H., Bundy, W., Harvey, C. (Eds.), *Kaolin genesis and utilization*. The Clay Mineral Society, Boulder, Colorado, pp. 261–290.
- Myers, P.G., Rohling, E.J., 2000. Modeling a 200-yr interruption of the Holocene sapropel S1. *Quat. Res.* 55, 98–104.
- Negri, A., Morigi, C., Giunta, S., 2003. Are productivity and stratification important to sapropel deposition? Microfossil evidence from late Pliocene i-cycle 180 at Vrica, 2002. *Palaeogeogr. Palaeoclimatol. Palaeoecol.* 190, 243–255.
- Nijenhuis, I.A., Brumsack, H.J., De Lange, G.J., 1998. The trace element budget of the eastern mediterranean during Pliocene sapropel formation. In: Robertson, A.H.F., Emeis, K.-C., Richter, C., Camerlenghi, A. (Eds.), *Proc. ODP Sci. Res.*, vol. 160. Ocean Drilling Program, College Station, TX, pp. 199–206.
- Nijenhuis, I.A., Bosch, H.-J., Sinninghe Damsté, J.S., Brumsack, H.-J., De Lange, G.J., 1999. Organic matter and trace element rich sapropels and black shales: a geochemical comparison. *Earth Planet. Sci. Lett.* 169, 277–290.
- Nijenhuis, I.A., Becker, J., De Lange, G.J., 2001. Geochemistry of coeval marine sediments in Mediterranean ODP cores and a land section: implications for sapropel formation models. *Palaeogeogr. Palaeoclimatol. Palaeoecol.* 165, 97–112.
- Okada, H., Honjo, S., 1973. The distribution of oceanic coccolithophorids in the Pacific. *Deep-Sea Res.* 20, 355–374.
- Olausson, E., 1961. Studies of deep-sea cores. *Rep. Swed. Deep-Sea Exped.*, 1947–1948 8, 323–438.
- Ozenda, P., 1975. Sur les étages de végétation dans les montagnes du bassin méditerranéen. *Doc. Cartogr. Écol.* 16, 1–32.
- Pescatore, T., Pozzuoli, A., Stanzone, D., Torre, M., Huertas, F., Linares, J., 1980. Caratteri mineralogici e geochimici dei sedimenti pelitici del Flysh di Gorgoglione (Lucania, Appennino meridionale). *Period. Mineral.* 49, 293–330.
- Pedersen, T.F., Calvert, S.E., 1990. Anoxia vs. productivity: what controls the formation of organic–carbon rich sediments and sedimentary rocks? *AAPG Bull.* 74 (4), 454–466.
- Peypouquet, J.P., 1977. Les ostracodes et la connaissance des paleomilieux profonds. Application au Cénozoïque de l’Atlantique nord-oriental. Ph.D. Thesis, Université Bordeaux, France.
- Prospero, J.M., Glaccum, R.A., Nees, R.T., 1981. Atmospheric transport of soil dust from Africa to South America. *Nature* 289, 570–572.
- Robertson, A.H.F., Emeis, K.-C., Richter, C., Camerlenghi, A. (Eds.), 1998. *Proceedings of the Ocean Drilling Program, Scientific Results*, vol. 160. Ocean Drilling Program, College Station, TX.
- Robinson, C., 1994. Lago Grande di Monticchio, southern Italy: a long record of environmental change illustrated by sediment geochemistry. *Chem. Geol.* 118, 235–254.
- Rohling, E.J., 1991. Shoaling of the Eastern Mediterranean pycnocline due to reduction of excess evaporation: implications for sapropel formation. *Paleoceanography* 6, 747–753.
- Rohling, E.J., 1994. Review and new aspects concerning the formation of eastern Mediterranean sapropels. *Mar. Geol.* 122, 1–28.
- Rohling, E.J., 2001. The dark secret of the Mediterranean — a case history in past environmental reconstruction. <http://www.soes.soton.ac.uk/sta1/ejr/DarkMed/ref-cond.html>.
- Rohling, E.J., Gieskes, W.W., 1989. Late Quaternary changes in Mediterranean intermediate water density and formation rate. *Paleoceanography* 4, 531–545.
- Rohling, E.J., Hilgen, F.J., 1991. The eastern Mediterranean climate at times of sapropel formation: a review. *Geol. Mijnb.* 70, 253–264.
- Rohling, E.J., de Stigter, H.C., Vergnaud-Grazzini, C., Zaalberg, R., 1993. Temporary repopulation by low-oxygen tolerant benthic foraminifera within an Upper Pliocene sapropel: evidence for the role of oxygen depletion in the formation of sapropels. *Mar. Micropaleontol.* 22, 207–219.
- Rohling, E.J., Jorissen, F.J., De Stigter, H.C., 1997. 200 year interruption of Holocene sapropel formation in the Adriatic Sea. *J. Micropaleontol.* 16 (2), 97–108.
- Rohling, E.J., Cane, T.R., Cooke, S., Sprovieri, M., Bouloubassi, I., Emeis, K.C., Schiebel, R., Kroon, D., Jorissen, F.J., Lorre, A., Kemp, A.E.S., 2002a. African monsoon variability during the previous interglacial maximum. *Earth Planet. Sci. Lett.* 202, 61–75.
- Rohling, E.J., Mayewski, P.A., Abu-Zied, R.H., Casford, J.S.L., Hayes, A., 2002b. Holocene atmosphere–ocean interactions: records from Greenland and the Aegean Sea. *Clim. Dyn.* 18, 587–593.
- Rohling, E.J., Hopmans, E.C., Sinninghe Damsté, J.S., 2006. Water column dynamics during the last interglacial anoxic event in the Mediterranean (sapropel S5). *Paleoceanography* 21, PA2018. doi:10.1029/2005PA001237.
- Rosignol-Strick, M., 1983. African monsoons, an immediate climate response to orbital insolation. *Nature* 304, 46–49.
- Rosignol-Strick, M., 1985. Mediterranean Quaternary sapropels, an immediate response of the African monsoon to variations of insolation. *Palaeogeogr. Palaeoclimatol. Palaeoecol.* 49, 237–263.
- Rosignol-Strick, M., Paterne, M., 1999. A synthetic pollen record of the eastern Mediterranean sapropels of the last 1 Ma: implication for the time-scale and formation of sapropels. *Mar. Geol.* 153, 221–237.
- Roth, P.H., Coulbourn, W.T., 1982. Floral and solutions patterns of coccoliths in surface sediments of the north Pacific. *Mar. Micropaleontol.* 7, 1–52.
- Sangiorgi, F., Capotondi, L., Combourieu Nebout, N., Vigliotti, L., Brinkhuis, H., Giunta, S., Lotter, A.F., Morigi, C., Negri, A., Reichert, G.-J., 2003. Holocene seasonal sea surface temperature variations in the South Adriatic Sea inferred from a multi-proxy approach. *J. Quat. Sci.* 18 (8), 723–732.
- Schmiedl, G., Mitschele, A., Beck, S., Emeis, K.C., Hemleben, C., Schulz, H., Sperling, M., Weldeab, S., 2003. Benthic foraminiferal record of ecosystem variability in the eastern Mediterranean Sea during times of sapropel S5 and S6 deposition. *Palaeogeogr. Palaeoclimatol. Palaeoecol.* 190, 139–164.
- Stefanelli, S., 2004. Cyclic changes in oxygenation based foraminiferal microhabitats: early–Middle Pleistocene, Lucania Basin (southern Italy). *J. Micropaleontol.* 23, 81–95.
- Stefanelli, S., Capotondi, L., Ciaranfi, N., 2005. Foraminiferal record and environmental changes during the deposition of the Early–Middle Pleistocene sapropels in southern Italy. *Palaeogeogr. Palaeoclimatol. Palaeoecol.* 216, 27–52.
- Subally, D., Quézel, P., 2002. Glacial or interglacial: Artemisia, a plant indicator with dual responses. *Rev. Palaeobot. Palynol.* 120, 123–130.
- Suc, J.-P., 1984. Origin and evolution of the Mediterranean vegetation and climate in Europe. *Nature* 307 (5950), 429–432.
- Suc, J.-P., Violanti, D., Londeix, L., Poumot, C., Robert, C., Clauzon, G., Turon, J.-L., Ferrier, J., Chikhi, H., Cambon, G., Gautier, F., 1995. Evolution of the Messinian Mediterranean environments: the

- Tripoli Formation at Capodarso(Sicily, Italy). Rev. Palaeobot. Palynol. 87, 51–79.
- Thomson, J., Higgs, N.C., Wilson, T.R.S., Croudace, I.W., De Lange, G.J., Van Santvoort, P.J.M., 1995. Redistribution and geochemical behaviour of redox-sensitive elements around S1, the most recent eastern Mediterranean sapropel. Geochim. Cosmochim. Acta 59, 3487–3501.
- Thunell, R.C., 1979. Pliocene–Pleistocene paleotemperature and paleosalinity history of the Mediterranean Sea: results from DSDP Sites 125 and 132. Mar. Micropaleontol. 4, 173–187.
- Thunell, R.C., Williams, D.F., Kennett, J.P., 1977. Late Quaternary paleoclimatology, stratigraphy and sapropel history in eastern Mediterranean deep-sea sediments. Mar. Micropaleontol. 2, 371–388.
- Tomadin, L., Lenaz, R., 1989. Eolian dust over the Mediterranean and their contribution to the present sedimentation. In: Leinen, M., Sarnthein, M. (Eds.), Paleoclimatology and Paleometeorology: Modern and Past Patterns of Global Atmospheric Transport. Kluwer Academic Publishers, pp. 267–282.
- Turekian, K.K., Wedepohl, K.H., 1961. Distribution of elements in some major units of the earth's crust. Bull. Geol. Soc. Am. 72, 125–192.
- van Harten, D., 1986. Use of ostracodes to recognize downslope contamination in paleobathymetry and a preliminary reappraisal of the paleodepth of the Prasas Marls (Pliocene), Crete, Greece. Geology 14 (10), 856–859.
- van Harten, D., 1987. Ostracodes and the early Holocene, anoxic event in the Eastern Mediterranean: evidence and implications. Mar. Geol. 75, 263–269.
- van Harten, D., 1995. Differential food-detection: A speculative reinterpretation of vestibule variability in *Kriithe* (Crustacea: Ostracoda). In: Riha, J. (Ed.), Ostracoda and Biostratigraphy. Balkema, Rotterdam, pp. 33–36.
- Vergnaud-Grazzini, C., 1985. Mediterranean late Cenozoic stable isotope record: stratigraphy and paleoclimatic implication. In: Stanley, D.J., Wezel, F.C. (Eds.), Geological evolution of the Mediterranean Basin. New York, pp. 413–451.
- Vergnaud-Grazzini, C., Ryan, W.B.F., Cita, M.B., 1977. Stable isotopic fractionation, climate change and episodic stagnation in the eastern Mediterranean during the late Quaternary. Mar. Micropaleontol. 2, 353–370.
- Von Breymann, M.T., Emeis, K.-C., Suess, E., 1992. Water depth and diagenetic constraints on the use of barium as a paleoproductivity indicator. In: Summerhayes, C.P., Prell, W.L., Emeis, K.C. (Eds.), Upwelling System: Evolution Since The Early Miocene. Geological Society Special Publication, vol. 64, pp. 273–284.
- Wehausen, R., Brumsack, H.-J., 2000. Chemical cycles in Pliocene sapropel bearing and sapropel barren eastern Mediterranean sediments. Palaeogeogr. Palaeoclimatol. Palaeoecol. 158, 325–352.
- Weldeab, S., Emeis, K.-C., Hemleben, C., Vennemann, T.W., Schulz, H., 2002. Sr and Nd isotope composition of Late Pleistocene sapropels and non-sapropelic sediments from the Eastern Mediterranean Sea: Implications for detrital influx and climatic conditions in the source areas. Geochim. Cosmochim. Acta 66, 3585–3598.
- Whatley, R., 1990. Ostracoda and global events. In: Whatley, R.C., Maybury, C. (Eds.), Ostracoda and Global Events. Chapman & Hall, London, pp. 3–24.
- Whatley, R., 1991. The platycopid signal: a means of detecting kenoxic events using Ostracoda. J. Micropaleontol. 10 (2), 181–185.
- Whatley, R., Zhao, Q., 1993. The *Kriithe* problem: A case history of the distribution of *Kriithe* and *Parakriithe* (Crustacea, Ostracoda) in the South China Sea. Palaeogeogr. Palaeoclimatol. Palaeoecol. 103, 281–297.
- Young, J.R., 1994. The functions of coccoliths. In: Winter, A., Siesser, W.G. (Eds.), Coccolithophores. Cambridge University Press, London, pp. 63–82.
- Ziveri, P., Thunell, R.C., Rio, D., 1995. Export production of coccolithophores in an upwelling region: results from San Pedro Basin, Southern California Borderlands. Mar. Micropaleontol. 24, 335–358.
- Ziveri, P., Rutten, A., de Lange, G.J., Thomson, J., Corselli, C., 2000. Present-day coccolith fluxes recorded in central eastern Mediterranean sediment traps and surface sediments. Paleogeogr. Palaeoclimatol. Paleoecol. 158, 175–195.
- Ziveri, P., Baumann, K.-H., Boeckel, B., Bollmann, J., Young, J., 2004. Biogeography of selected Holocene coccoliths in the Atlantic Ocean. In: Thierstein, H.R., Young, Y.R. (Eds.), Coccolithophores from Molecular Processes to Global Impact. Springer, Berlin, pp. 403–428.